Modelling, simulation and evaluation of ground vibration caused by rail vehicles

State-of-the-art review for 26th IAVSD Symposium, Gothenburg, Sweden, August 2019

David J. Thompson[a*], Georges Kouroussis[b] and Evangelos Ntotsios[a]

[a]Institute of Sound and Vibration Research, Faculty of Engineering and the Environment, University of Southampton, Southampton SO17 1BJ, United Kingdom; [b]Faculty of Engineering, Department of Theoretical Mechanics, Dynamics and Vibrations, Université de Mons — UMONS, Place du Parc 20, B-7000 Mons, Belgium

ABSTRACT
There is a great need to develop rail networks over long distances and within cities as more sustainable transport options. However, noise and vibration are seen as a negative environmental consequence. Compared with airborne noise, the related problem of ground vibration is much more complex. The properties of the ground vary significantly from one location to another. There is no common assessment criterion or measurement quantity and no equivalent to the noise maps. Ground-borne vibration is transmitted into buildings and perceived either as feelable whole-body vibration or as low frequency noise; it can also affect sensitive equipment but it is generally at a level that is too low to cause structural or cosmetic damage to buildings. A review is given of evaluation criteria for both feelable vibration and ground-borne noise, empirical and numerical prediction methods, the main vehicle and track parameters that can affect the vibration levels and a range of possible mitigation methods.

KEYWORDS
railway vibration; vehicle/track interaction; environmental assessment; ground-borne noise; structural vibration; transition zone

1. Introduction

Railways are generally seen as an environmentally friendly and sustainable form of transport. Increasing the market share of rail transport for both passengers and freight is therefore seen as having positive effects on the environment, reducing congestion as well as air pollution and greenhouse gases. In [1] the EU states an aim of achieving a shift of 50% of road freight journeys over 300 km to rail and water by 2050, while the majority of medium distance passenger transport should go by rail.

Despite these environmental benefits, however, noise and vibration have for many years been seen as a negative environmental consequence of rail, as well as other forms of transport. Noise is often the main reason for objections from residents to new railways and complaints about existing lines have also increased. In response to public concern about noise pollution, noise maps have been introduced across Europe as well as common assessment criteria for environmental noise [2].

More recently the related problem of ground vibration has also come to be seen as an important environmental impact of railways. Compared with airborne noise, ground vibration is much more complex as the medium through which the vibration propagates is inhomogeneous, with properties that vary significantly from one place

to another. There is no common assessment criterion or measurement quantity and no equivalent to the noise maps.

Vibration is generated at the wheel/rail interface as indicated in Figure 1. As the wheel moves along the rail the steady axle loads and the dynamic forces induced by wheel/rail unevenness cause vibration of the track and the underlying soil. As shown in Figure 2, this vibration propagates from both surface and underground railways through the soil to neighbouring buildings. To understand the generation and propagation of vibration requires knowledge of wheel/rail dynamic interaction, soil dynamics, soil-structure interaction, and structural vibration.
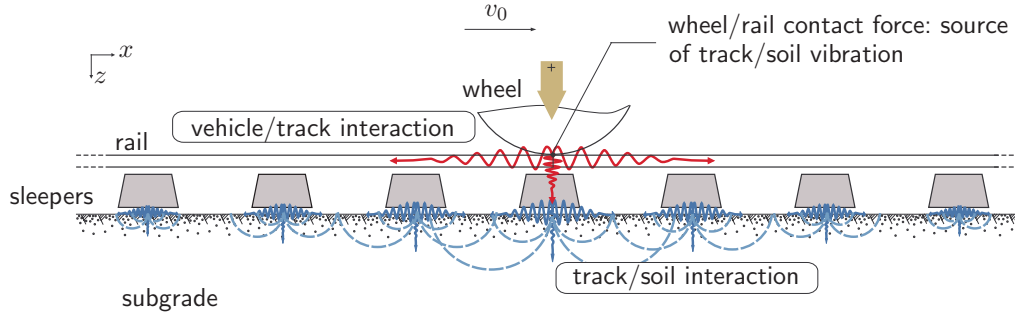

Figure 1. Wheel/rail and sleeper/subgrade interactions

Vibration is perceived by humans in two different ways. At low frequencies people are sensitive to whole-body vibration, whether they are standing, sitting or lying down. The relevant frequency range for this feelable vibration is limited to 1-80 Hz. In addition, vibration inside buildings leads to low frequency acoustic radiation which is heard as a rumbling noise. The relevant frequency range for this ground-borne noise is approximately 20-250 Hz. In practice both phenomena occur simultaneously. Moreover, rattling of windows, doors or furnishings can also occur. In almost all cases railway-induced vibration is at a level which is far too low to cause structural or cosmetic damage to buildings [3]. However, in addition to its effect on humans, vibration can also be important for the functioning of sensitive equipment.

The paper sets out to give a detailed review of the criteria used to evaluate ground vibration, the modelling and simulation of railway ground vibration and the means available to control it.

2. Evaluation of ground vibration

2.1. *Criteria for feelable vibration*

In order to quantify the effects of vibration on humans and buildings, several recommendations and guidelines exist, based on measurement and interpretational methodologies. Most often, frequency weighting curves are specified, based on a kind of transfer function between excitation and feelable response [4]. Detection threshold curves are derived from such weighting curves and take the name of iso-perception curves in the case of human response to vibration (comfort).

In the case of negative effects caused by railway induced ground vibration, two main categories of feelable vibration are recognized:

- whole-body vibration, in the frequency range 1–80 Hz,
- effects on structures/buildings, usually at low frequencies, including sensitive equipment inside buildings.
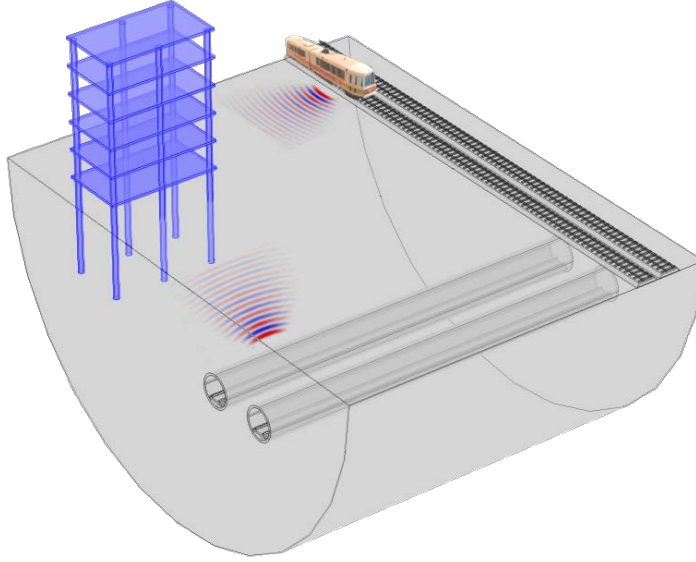
Figure 2. Ground-borne vibration and noise concept.

Standards are available to specify the allowable vibration levels, based on the analysis of dedicated vibration indicators. Several standards and guidelines are available, which define adequate procedures and assessments. The most important ones are:

- the international standards ISO 2631 [5, 6], which are often considered as a reference for comfort evaluation,
- the British Standards BS 6841 [7] and BS 6472-1 [8] considered as very similar to the aforementioned international standards,
- the international standard ISO 4866 [9], for measurement and processing data with regard to evaluating vibration effects on structures,
- the German standards DIN 4150-2 [10] and DIN 4150-3 [11] which are also used beyond the borders including in UK, Belgium and other European countries,
- the Swiss standards SN 640 312a [12] dealing with building damage only,
- the Norwegian standard NS 8176 [13] for comfort assessment,
- the recommendations [14, 15] of the United States Department of Transportation (USDOT) for the assessment of potential vibration impacts resulting from high-speed train lines and mass transits.

2.1.1. Primary indicators

Trace velocities and accelerations are often used as primary indicators. Since a vibration signal is complicated by nature, single value estimators are usually retained.

A root mean squared (rms) value is recommended by [6, 7] to describe the smoothed vibration amplitude by supposing that the human body responds to an average vibration amplitude during a recorded time $0 \leq t \leq T$

$$\langle \mathrm{a}_w \rangle = \sqrt{\frac{1}{T} \int_0^T a_w^2(t)\, \mathrm{d}t} \tag{1}$$

where the weighted acceleration a_w is derived from the time history of the acceleration $a(t)$. According to the standards, the weighting function $W(f)$ may differ. In the case of evaluations inside buildings [6], one single filter is defined, independent of the measurement direction and human position, focusing on the frequency range 1-20 Hz. Because vibration is often non-stationary, the DIN 4150-2 standard [10]

suggests the use of a running root mean square instead of a classical root mean square, for which the signal duration affects the calculated value. Moreover, the velocity signal is used as the primary indicator and is passed through a high-pass filter (cut-off frequency of 5.6 Hz). The weighted time-averaged signal is defined:

$$KB_F(t) = \sqrt{\frac{1}{\tau} \int_0^t KB^2(\xi)\, e^{-\frac{t-\xi}{\tau}}\, \mathrm{d}\xi} \tag{2}$$

where $KB(t)$ is the weighted velocity signal. The integration time τ for the averaging is equal to 0.125 s.

Considering that vibrations consist of rapidly fluctuating motions, a decibel scale is often preferred

$$V_{dB} = 20 \log_{10} \frac{v_{rms}}{v_{ref}} \tag{3}$$

where v_{rms} is the root mean square amplitude of the velocity time history and v_{ref} is the reference value. There is no common standard for v_{ref}, with $5 \cdot 10^{-8}$ m/s, 10^{-9} m/s and 10^{-6} in/s [15] all being used.

Peak values are also retained, especially for evaluating the effect of vibration on buildings. The peak particle velocity PPV, defined as the maximum absolute amplitude of the velocity time signal, is used in several standards but with slightly different definitions:

- The DIN 4150 standard [11] suggests that, if multiple directions are measured, the maximum of the three components is retained

$$PPV = \max(v_x, v_y, v_z) \tag{4}$$

  where v_x, v_y, v_z are the x-, y- and z- components of the velocity vector.
- The Swiss standard [12] also uses a PPV but it is defined as the norm of the vector velocity

$$PPV = \sqrt{v_x^2 + v_y^2 + v_z^2}\,. \tag{5}$$

The rms acceleration and PPV do not take account of the number or duration of events. To account for this, in BS 6472 [8] a "vibration dose value" (VDV) is introduced which is defined as

$$VDV = \left[\int_0^T a_w^4(t)\,dt \right]^{0.25} \tag{6}$$

where $a_w(t)$ is the filtered acceleration (using W_b for vertical vibration as defined in BS 6472 [8]) and T is the duration of the event. The total VDV for a number of events can be obtained using

$$VDV_T = \left[VDV_1{}^4 + VDV_2{}^4 + VDV_3{}^4 + ... \right]^{0.25} \tag{7}$$

The VDV is much more strongly influenced by the vibration level than the duration. For N identical events, from Eq. (7), $VDV_T = VDV \cdot N^{0.25}$ which implies that to halve the VDV for a train service would require a reduction of the number of events by a factor of 16.

The VDV can be compared with broad criteria for acceptability [8]. For railway projects it is usual to work to a limit of avoiding the "low probability of adverse comment", which in residential buildings corresponds to a VDV of less than 0.2 m/s$^{1.75}$ over a 16 hour day and 0.1 m/s$^{1.75}$ over an 8 hour night. Although ISO 2631-1 also contains the VDV method, ISO 2631-2, of direct relevance to building vibration, does not.

To determine the VDV the measured time histories of vibration are required. If only rms values or frequency spectra are available, an estimate of the VDV ($eVDV$) can be obtained [8] although there can be large variations between this and the true VDV.

2.1.2. Effect on buildings and whole-body vibration

For the vibration perception, ISO 14837-1 [16] refers to ISO 2631-1 for the evaluation, using the acceleration as primary indicator, although for the damage effects on buildings, ISO 4866 [9] is cited, working with the particle velocity as indicator. People have widely differing perception thresholds for whole-body vibration. According to [8] about half of people can perceive a vertical weighted vibration with a peak acceleration of 0.015 m/s^2, based on the W_b weighting [8] (i.e. rms of about 0.01 m/s^2).

A number of limit curves are defined as part of the detailed vibration assessment in [14, 15]. These are redrawn in Figure 3 in terms of dB re 10^{-9} m/s. Vibration spectra should be compared with these curves to ensure that they do not exceed the relevant limit curve. The curve labelled "Residential (night)" corresponds to one-third octave levels of 100 dB, or 0.1 mm/s rms over the range 8-80 Hz. This was defined in earlier versions of ISO 2631-2 (1989) and BS 6472 (1992) as a "base curve", corresponding approximately to the average threshold of perception. The curves labelled VC-A to VC-E are intended as limit curves for different types of vibration-sensitive equipment such as microscopes.
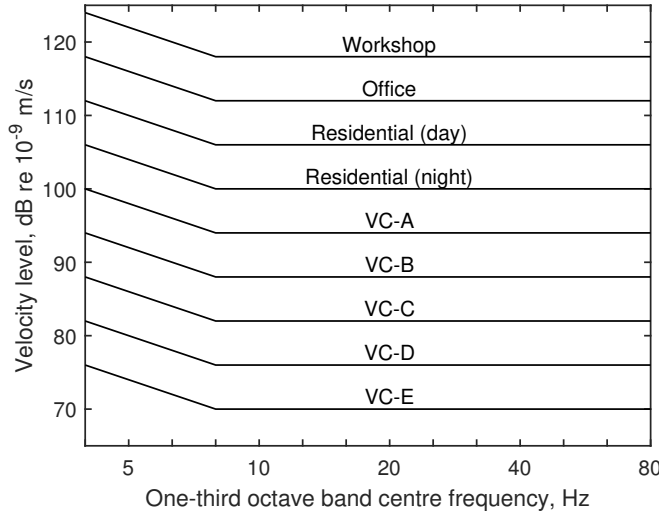

Figure 3. Criteria for detailed vibration analysis, replotted from [14, 15].

The undesirable and unpleasant adverse side effects of the whole body vibration are not exclusively limited to comfort issues, but also to other disturbances, including health problems [17].

Regarding Eq. (2), a first evaluation suggested by DIN 4150-2 [10] is assessed by comparing the maximum level $KB_{F,\mathrm{max}} = \max(KB_F(t))$ with two guideline limits

denoted A_u and A_o, for a whole evaluation and for the short-term vibration as well. Table 1 gives guideline values for the evaluation of human exposure to vibration in dwellings and similarly used spaces. When $KB_{F,\mathrm{max}}$ is between the lower and upper limits A_u and A_o, it is necessary to estimate further indicators to be compared to the third guideline limit A_r, to take account of the number of events.

Table 1. Guideline values for evaluating human exposure to vibration in dwellings and similar spaces (A_u: lower limit, A_o: upper limit, A_r: value for comparison with $KB_{F,Tr}$ values) [10]

Category	Location of building	Day/Night		
		A_u	A_o	A_r
1	Buildings in purely industrial areas, where the only dwellings are intended for plant owners or managers, superintendents, stand-by service personnel, ...	0.4/0.3	6/0.6	0.2/0.15
2	Buildings in predominantly commercial areas	0.3/0.2	6/0.4	0.15/0.1
3	Buildings in areas which are neither predominantly commercial nor predominantly residential	0.2/0.15	5/0.3	0.1/0.07
4	Buildings in areas which are predominantly or purely residential	0.15/0.1	3/0.2	0.07/0.05
5	Buildings in specially protected areas (such as hospitals) or in health resorts	0.1/0.1	3/0.15	0.05/0.05

Specifically for rail traffic:

- Underground rail traffic: the A_u and A_r values in Table 1 apply for all types of underground rail traffic.
- Surface urban transportation: for this type of rail traffic, the A_u and A_r values shall be multiplied by a factor of 1.5.
- Surface traffic other than urban transportation: a small overrun is sometimes allowed, e.g. for historical or human factors.

Only ISO-4866 [9], DIN 4150-3 [11] and the Swiss standard [12] give building damage assessment methods, relating the PPV to the structural stress. The German and Swiss standards are solely dedicated to the effect on the structure and provide threshold values, often called Z-curves, as a function of the building type, the location inside the building (at the foundation or in the plane of the highest floor) and the nature of vibration (short- or long-term vibration in [11]; occasional, frequent or continuous excitation in [12]). Figure 4 displays the associated limits, showing that they are close to each other. The Swiss standard has the advantage to consider explicitly the frequency of events (cumulative damage). It is also observable that the DIN limits are approximately close to the Swiss limits for frequent-to-continuous excitations. It is noteworthy that, for both standards, if the limit is reached, additional evaluation procedures are recommended, based on advanced technical measurement (safety step). However for rail traffic the vibration levels are rarely of concern for structural damage.

2.1.3. On the interest of dedicated methods for railway traffic

In view of these different ways of estimating vibration perception and allowable vibration levels in buildings, thresholds may differ significantly and contradictory recommendations can be provided by different guidelines. This was confirmed in [18] by analysing practical results based on mono-frequency excitation and railway-induced ground vibration. In the same context, Ainalis et al. [19] analysed the DIN 4150-3 standard and proposed an improved analysis: having in mind that a
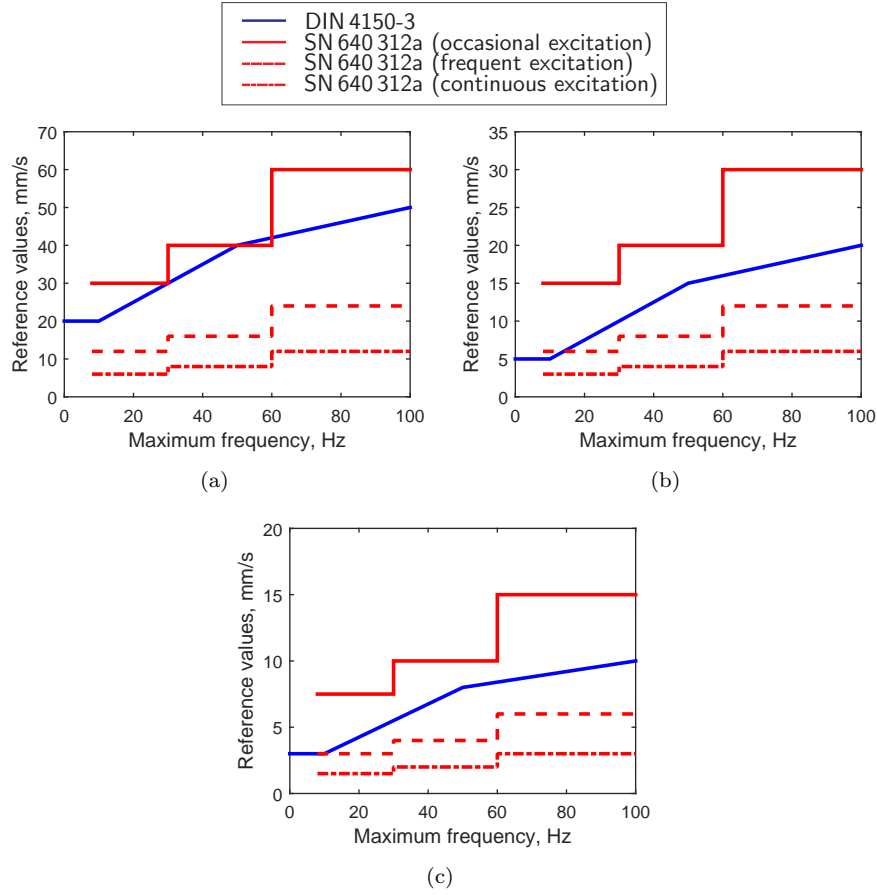
Figure 4. Comparison between DIN 4150-3 and SN 640 312a for the effects on building according to the type of structure [18]: (a) industrial buildings, (b) standard buildings and (c) sensitive buildings

ground vibration trace is non-stationary by nature, they suggested to use a time-frequency distribution based on the continuous wavelet transform to accurately identify the level and frequency content of a ground vibration signal. Figure 5 illustrates these observations by presenting the DIN 4150-3 Z-curves (Figure 4) with localised estimates of the PPV and dominant frequency. It is observed that the dominant frequency does not always correspond to the frequency content in the vicinity of the magnitude maximum. This can be explained by the uncertainty principle in Fourier analysis according to which the minimum frequency bandwidth increases as the time window is reduced [20]. This is also more pronounced for the passing of a railway vehicle on a localized defect than for the passing of a railway vehicle on a rough rail.

Waddington et al. [22] conducted a large scale experimental analysis to deliver guidance on the evaluation of human response to vibration from railways in residential environments close to freight lines with the aim of achieving a harmonization of assessment methods, including human perception, evaluation methods, annoyance, sleep impacts and non-exposure factors.

2.2. Criteria for ground-borne noise

In common with environmental noise, it is usual to assess ground-borne noise in terms of the A-weighted sound pressure level in decibels. The A-weighting filter attempts to mimic human sensitivity to sound at relatively low amplitudes but is widely used in assessing noise at all amplitudes. This filter attenuates the sound
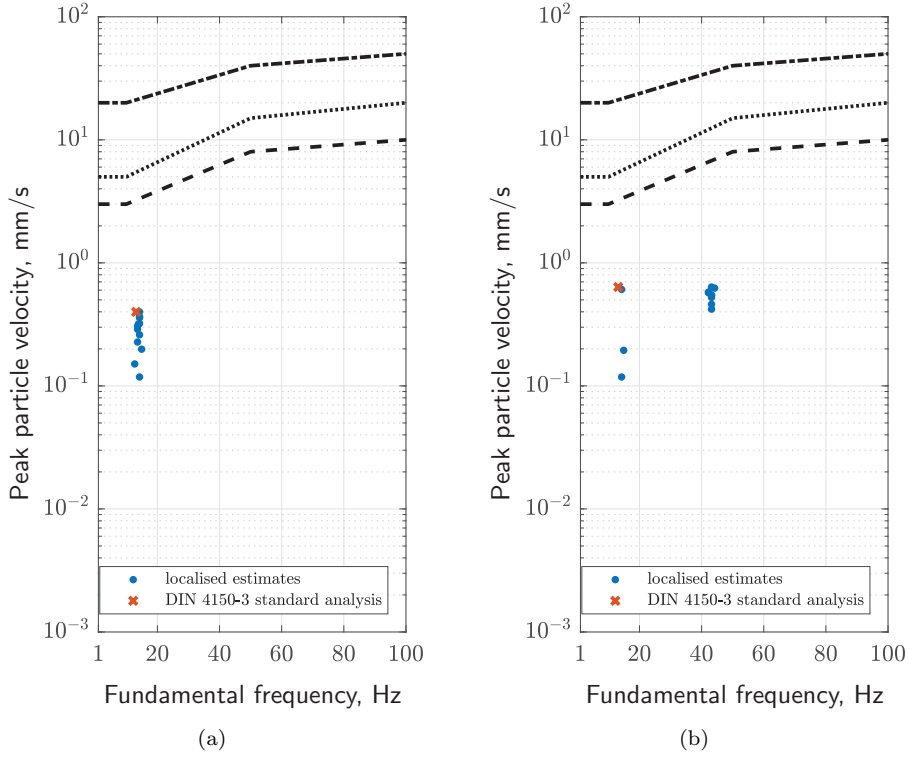
Figure 5. Analysis of the train-induced ground vibrations (results from [21]) using the continuous wavelet transform to compute localised estimates of the PPV and dominant frequency, presented on a DIN 4150-3 Z-curve: (a) passing of an InterCity train on a rough rail and (b) passing of an InterCity train on a track with a rail joint

pressure levels below 100 Hz by more than 20 dB and the level at 20 Hz by as much as 50 dB.

In order to quantify the magnitude of a fluctuating sound pressure p, it is conventional to use the mean-square value over a time T

$$\bar{p^2} = \lim_{T \to \infty} \frac{1}{T} \int_{t_1}^{t_1+T} p^2(t)dt \tag{8}$$

in which t_1 is an arbitrary time. The sound pressure level in decibels is defined by

$$L_p = 10 \log_{10} \left(\frac{\bar{p^2}}{p_{ref}^2} \right) \tag{9}$$

where p_{ref} is the reference pressure which usually takes the value of 20 µPa. In practice, in a sound level meter an exponential time weighting is used to allow a continuous reading of the sound pressure level

$$L_{p\tau} = 10 \log_{10} \left(\frac{1}{\tau} \int_0^\infty \frac{p^2(t-u)}{p_{ref}^2} e^{-u/\tau} du \right) \tag{10}$$

in which τ is the time constant. This is usually set to 0.125 s for fast (F) weighting or 1 s for slow (S) weighting. In practice the infinite limit can be truncated to a suitable finite time.

Ground-borne noise is expressed either in terms of the long-term average A-weighted sound level, L_{Aeq}, or the maximum sound level during a train passage.

For the latter usually the slow time constant is used, this being written as L_{ASmax} [16]. In the UK and US only the maximum level is considered whereas in the Netherlands, Spain and Switzerland only the equivalent sound level is used; in other countries such as Austria, Norway and Sweden both measures are used together and separate criteria set for each [23]. In Norway and Sweden the fast time constant is used. L_{AFmax} will be typically 1-2 dB higher than L_{ASmax} for continuously welded track and 3-4 dB higher for jointed track [16].

Measurement procedures for vibration and ground-borne noise inside buildings are set out in [24]. In [16] it is recommended that the sound pressure level should be measured near (but not at) the centre of the room. Due to the presence of distinct room modes at low frequencies, the sound pressure level near the walls may be 2-3 dB higher than this [16] but with variations of up to 10-20 dB at certain frequencies [23].

Different criteria for acceptable levels apply in different countries and these often depend on the use of the building. Criteria for maximum sound pressure levels L_{Amax} vary between 30 and 45 dB, while those for equivalent sound levels L_{Aeq} vary between 25 and 40 dB [23]. These criteria mostly apply only to new railway projects or where a substantial change of use is planned.

Although separate criteria are set for feelable vibration and ground-borne noise, some studies have dealt with human responses to railway noise combined with railway induced vibration, showing that vibration leads to greater noise annoyance [25]. Results of a recent laboratory experiment [26] suggest that the total annoyance caused by combined noise and vibration is considerably greater than the annoyance caused by noise alone. Further studies are required to link the results from field surveys with the laboratory experiments.

2.3. *Empirical methods for estimating ground vibration*

The most common internationally-used methodology for railway vibration assessment, for either new railway lines or new buildings adjacent to existing railways, is based on in-situ tests carried out before construction starts [27, 28]. This is defined in the Detailed Vibration Assessment (DVA) procedure of the U.S. Federal Railroad Administration (FRA) [14] and the Federal Transit Administration (FTA) [15]. The procedure is based on a technique for separate characterization of the source and the vibration propagation, developed in [29, 30]. This empirical methodology was been used in many countries since the 1980s.

The source is defined as a line of incoherent point forces located along the railway alignment; it is expressed as a line force density. The vibration propagation is defined as a transfer function from a line force density of unit amplitude to the vibration velocity at a certain distance from the alignment. This transfer function is expressed as a line-source transfer mobility, which is determined by combining point-source transfer mobilities measured from a series of points along the alignment [14]. These are measured by exciting the ground using a large hammer or dropped-weight.

To determine the force density, measurements of vibration are taken at a certain distance from the track during train passages. The line-source transfer mobility is then measured from the railway alignment to the same receiver location. From the ratio of these the force density can be inferred [14].

For the case of a proposed new line or tunnel, ground transfer functions are measured from the proposed location of the track to determine the vibration propagation characteristics of the soil and transmission into buildings (Figure 6(a)). The predicted vibration levels are then calculated by combining these characteris-

tics with the expected train excitation forces during future operation. These forces are often estimated from measurements at other locations which may then be adjusted by results from calculation models to allow for differences in, for example, vehicle or track properties.
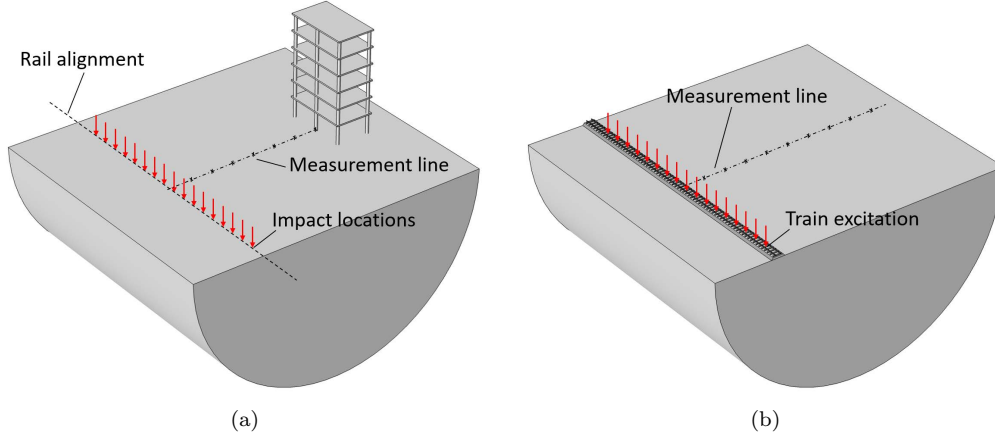

Figure 6. Typical experimental setups for evaluating soil/building transfer function [14]: (a) for the case of a new line and (b) for the case of a new building.

When a new building is planned near an existing operational line, a similar technique can be used to estimate the levels of vibration and re-radiated noise in the proposed building. In this case, the characterisation of the vibration source can be performed more accurately, since vibration measurements can be made during the operation of trains on the existing line and used to estimate the vibration levels at the proposed location of the new building (Figure 6(b)). However, in this case there is no available measured information about the vibration propagation from the soil into the building. Moreover, due to soil-structure interaction the actual response when the building is constructed could differ significantly from the measured ground response in the absence of the building. This difference is called the "coupling loss" [14, 24].

In the FRA procedure, generic building adjustment factors are suggested to account for ground-building foundation interaction and the amplification or attenuation of vibration levels through the building ("building transmissibility") [14, 24]. These adjustment factors contain a large uncertainty range. Moreover, the measurements used to establish them [30] were obtained in North America in the 1970s and so their relevance to modern buildings in other locations is questionable. In addition, they cannot be used with sufficient accuracy for buildings with unusual foundations and/or in untypical geological conditions. The validity and accuracy of the FRA/FTA procedure has been studied by a number of authors using theoretical models [31–35].

To estimate the sound pressure level from the vibration level on the floor a simple estimate given by Kurzweil [36] is often used:

$$L_p = L_v + C \tag{11}$$

where L_v is the velocity level and C is in dB. If the velocity level is expressed relative to $5 \cdot 10^{-8}$ m/s, $C = 7$ dB, whereas if the reference of 10^{-9} m/s is used it becomes $C = -27$ dB. In reality the dependence is frequency-dependent and recent evidence suggests Eq. (11) may give conservative estimates [37], which may be

more representative of the average in the room than the level near the centre of the room [38]. A more detailed procedure is also given by [38].

A specific empirical procedure was developed by Hood et al. [39] for the assessment and calculation of feelable vibration and ground-borne noise from the operation of trains in railway tunnels in London. In this model, the vibration due to a moving train was assumed to reduce with increasing distance from the tunnel and was derived from multiple regression over a large set of measured data. Source terms were measured on French high-speed trains. A chain of transmission losses within the source-path-receiver system was applied to enable the approach to be applied to a variety of planning situations. Similar empirical methods have been developed for use in Switzerland [40] and Scandinavia [41].

3. Modelling of ground vibration

Modelling ground-borne noise and vibration from railways is essential for understanding the physics of its generation and propagation. A good understanding is important in identifying ways to tackle unacceptable levels of vibration from existing as well as future railway lines. Railway induced noise and vibration in buildings (Figure 2) is a complex three-dimensional (3D) coupled problem, involving moving loads and dynamic soil-structure interaction at both the source (the railway) and the receiver (the building where vibration is perceived). Usually, "weak coupling" between source and receiver is assumed leading to a two-step procedure, where the free-field ground response due to a running train is calculated first and then it is used for predicting the building response, assuming that the presence of the building does not affect the vehicle /track interaction. In this section, the attention will be given to the wave propagation in the soil, as well as on the prediction of the free-field ground response whereas much less attention is given to the building response.

In the field of railway ground-borne vibration, the soil is most often modelled by assuming linear elastic constitutive behaviour. This arises from the fact that during the passage of a train, the strain levels in the soil remain relatively low apart from a small zone close to the track. For the track subgrade, where large strains (i.e. between 10^{-4} and 10^{-2}) are expected, the non-linear behaviour can be included in an equivalent linear analysis by assuming stiffness degradation and increased energy dissipation under large amplitude cyclic loading [42, 43].

Waves may propagate within an infinite elastic homogeneous and isotropic medium (usually referred as a full-space) in two fundamental wave types. Dilatational or longitudinal waves, involving no rotation, propagate at c_p while shear waves, which are transverse waves involving no volume changes, propagate at c_s. These wave speeds are given by

$$c_p = \left(\frac{\lambda + 2\mu}{\rho}\right)^{\frac{1}{2}} \text{ and } c_s = \left(\frac{\mu}{\rho}\right)^{\frac{1}{2}} \tag{12}$$

where μ is the shear modulus (or second Lamé coefficient) and λ is the first Lamé coefficient which is related to μ and the Poisson's ratio ν by

$$\lambda = \frac{2\mu\nu}{1 - 2\nu}. \tag{13}$$

The ratio of the two speeds may be expressed as

$$\alpha = \frac{c_s}{c_p} = \left(\frac{\lambda + 2\mu}{\mu}\right)^{\frac{1}{2}} = \left(\frac{1 - 2\nu}{2 - 2\nu}\right)^{\frac{1}{2}} \tag{14}$$

Since $0 \le \nu \le \frac{1}{2}$, $c_s < c_p$. Regarding the energy dissipation in the soil under cyclic excitation, it has been found that for low frequencies it is generally frequency independent and hysteretic material damping in the soil can be modelled in the frequency domain through the use of a complex shear modulus μ^* and a complex dilatational modulus $(\lambda + 2\mu)^*$ by introducing a factor $(1 + i\eta)$ where η is the damping loss factor or $(1 + 2i\xi)$ where ξ is the damping ratio.

A variety of terminology exists in the technical literature for the two wave types. Dilatational waves are also called longitudinal, irrotational and primary (P-) waves. The shear waves are also called rotational, transverse, equivoluminal, distortion and secondary (S-) waves.

3.1. *Wave propagation in a semi-infinite medium*

A ground that has a free surface is often idealized simply as a half-space (or semi-infinite domain) of homogeneous and isotropic elastic material. At the free surface of a half-space, interaction between dilatational and shear waves results in a surface wave or "Rayleigh" wave [44]. The Rayleigh wave propagates along the free surface by elliptical motions of the soil particles with growing amplitude towards the surface. Similarly to the P-wave and the S-wave, the Rayleigh wave in a half-space is non-dispersive, meaning that its speed does not vary with frequency. It is the slowest wave of the half-space, having a speed between 87% and 95% of the shear wave speed (depending on the Poisson's ratio of the material) [45]:

$$c_R \approx \frac{0.862 + 1.14\nu}{1 + \nu} c_s \tag{15}$$

It is the Rayleigh wave that usually carries the greatest part of the wave energy that is transmitted, particularly to larger distances along the surface.

However, all grounds are stratified on some scale and this layered structure of the ground has important effects on the propagation of surface vibration in the frequency range of interest. Typically, grounds have a layer of softer *weathered* material that is only about 1 to 3 metres deep on top of stiffer soil layers or bedrock, depending on the geology of each site. In such a layered ground medium, vibration propagates parallel to the surface via a number of wave types or modes. These are often called Rayleigh waves of different orders (R-waves) and Love waves. The Rayleigh waves are also called P-SV waves since they involve coupled components of dilatational deformation and vertically polarized shear deformation. Here the name P-SV wave is preferred and the term Rayleigh wave is reserved for the single such wave that exists in a homogeneous half-space. Love waves are decoupled from these and only involve horizontally polarized shear deformation and so are also known as SH waves. Since the vertical forces in the track dominate the excitation of vibration in the ground, the SH waves are not strongly excited and usually are ignored in the calculations of ground vibration from railways.

To illustrate, a measured example of P-SV surface waves is shown in Figure 7 for a test site near Wolverhampton (UK). This is derived from frequency response measurements obtained at a set of points on the ground surface at different distances from the excitation, in this case applied by a large hammer. The responses

at different distances are then Fourier transformed to express them in terms of wavenumber ($k = 2\pi/\lambda$ with λ the wavelength) at each frequency [46] (Figure 7(a)). The phase velocity of each wave at a particular frequency is given as the ratio of the frequency to the wavenumber ($c = \omega/k$; Figure 7(b)). For visualization purpose, the response shown in Figure 7(a) and Figure 7(b) is normalized with the maximum response measured at that frequency. Each peak in the diagrams represents a wave type associated with a cross-sectional mode of the soil. It can be seen that at low frequencies (below 15 Hz), the fundamental surface wave has a quite high phase velocity, corresponding to the phase velocity of P-SV waves in the underlying stiff ground layers. At high frequencies, the phase velocity converges asymptotically to a value of about 170 m/s in this example, corresponding to the Rayleigh wave localised in the top layer of soil.
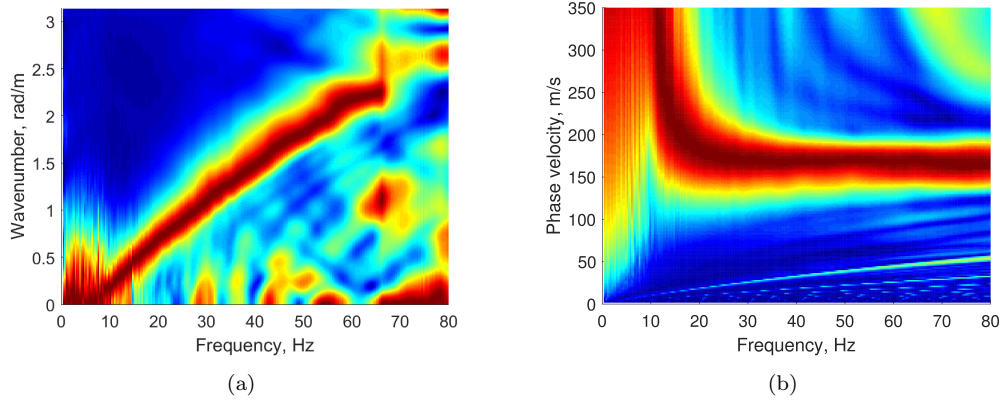

Figure 7. P-SV wave modes measured for a site near Wolverhampton, UK: (a) dispersion diagram; (b) phase velocity plot.

To model a stratified ground, a half-space of homogeneous and isotropic elastic layers can be used. There are several approaches for modelling a layered half-space in the literature. These are based mainly on the flexibility matrix method [47, 48] (known also as Haskell-Thomson transfer matrix method), or its alternative formulation, the dynamic stiffness matrix method [49]. Using such a semi-infinite layered medium model, the wave propagation can be calculated and the dispersion and attenuation properties can be estimated by the solution of an eigenvalue problem [50–52]. This eigenvalue problem is transcendental and has an infinite number of solutions, and must be solved with search techniques. This procedure is computationally expensive and sometimes it can lead to local optima or unidentifiability issues.

An example of the characteristic curves of the waves that propagate at the surface of a ground, modelled as a soft layer of weathered soil overlying a stiffer substratum of material, is shown in Figure 8. For the calculated results presented, the soft soil is a 3 m deep layer and its material properties are given in Table 2.

Table 2. Properties used for the ground model in Figure 8.

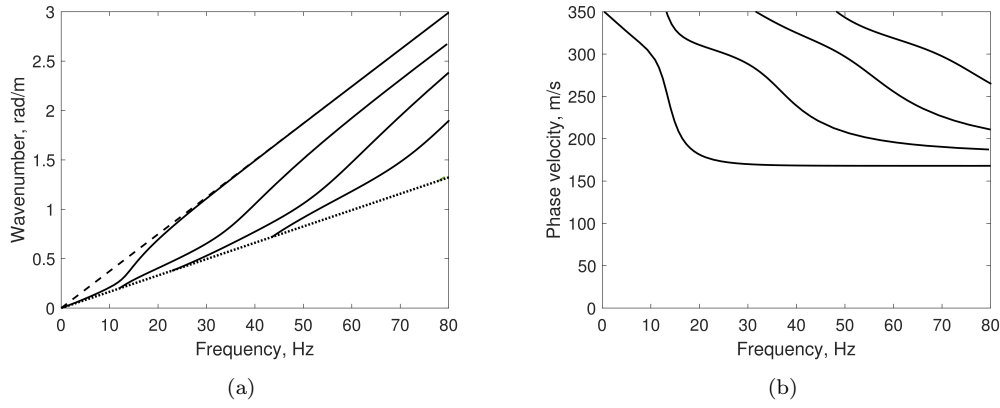|	Surface layer	Underlying half-space
S-wave speed	180 m/s	380 m/s
P-wave speed	360 m/s	700 m/s
Density	1700 kg/m^3	2000 kg/m^3
Damping loss factor	0.1	0.3

Figure 8. (a) Characteristic curves for (———) propagating P-SV waves of a layered half-space: (a) dispersion diagram with (– – –) Rayleigh wave of the upper layer material and (· · · ·) shear wave of the underlying half-space; (b) phase velocity plot.

Since the ground modelled in Figure 8 is not homogeneous, the P-SV waves are dispersive, meaning that the phase velocity (and the attenuation coefficient, not presented here) of the waves varies with frequency. Figure 8(a) presents the dispersion diagram for the example ground where the wavenumber is plotted as a function of frequency. For comparison, the Rayleigh wave speed of a homogeneous half-space corresponding to the upper material and the S-wave speed of the underlying soil type are also shown in Figure 8(a). Each line of the diagram represents a wave type associated with a cross-sectional mode of the layered soil. The corresponding phase velocities are shown in Figure 8(b).

The phase velocity of the dispersive surface modes can also be derived from the wavenumber content of the responses of the layered half-space due to a unit harmonic force. These are shown in the contour plots of Figure 9(a) and 9(b) for the example ground model discussed earlier. In Figure 9(a), for each frequency, the amplitude of the vertical response is plotted against radial wavenumber. Similarly with the measured responses shown in Figure 7(b), the calculated response shown in Figure 9(b) is normalized with the maximum response measured in each frequency. The wavenumber content of the responses exhibits peaks that reveal the presence of the P-SV waves. The largest peak corresponds to the dominant surface wave. It can be seen that although the contour plot cannot identify all surface waves of the layered half-space, it can identify the surface wave that dominates the response.
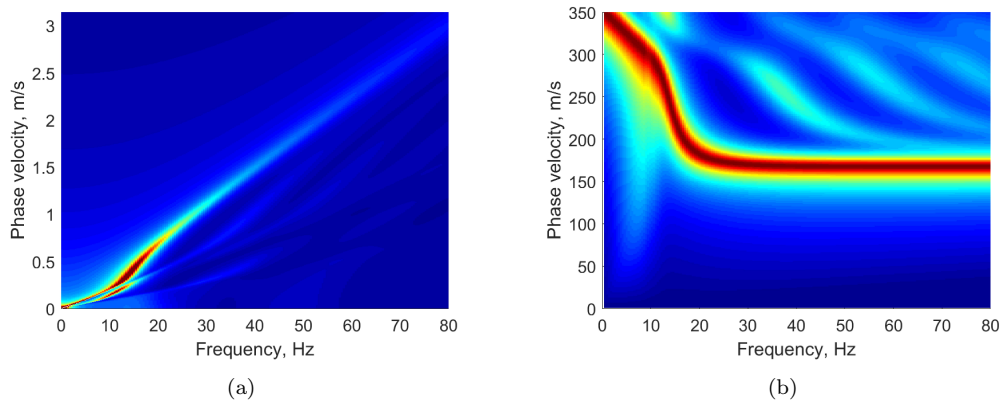

Figure 9. (a) Contour plot of the vertical displacement (m/N) (a) in the frequency-wavenumber domain and (b) phase velocity versus frequency plot.

For this example set of soil parameters, at very low frequency, only a single mode exists and this has a wave speed close to that of the shear waves in the substratum. Around 15 Hz, the depth of the weathered material sustains a quarter wavelength of the shear wave. Above this frequency, waves propagate in the upper layer with little influence of the underlying soil. With the onset of this mode, i.e. propagation via the layer material, a rise in the transmitted level of vibration is observed in Figure 9(a). For the cases of regular ground types in which stiffness increases with depth, this is the fundamental P-SV wave. At high frequency, as the wavelengths become small compared with the depth of the weathered material layer, the wavenumber of the slowest wave converges towards that of the Rayleigh wave in a half-space of the upper layer material that is estimated about 168 m/s. Higher order propagating waves "cut on" at frequencies of 12 Hz, 23 Hz and 43 Hz (Figure 8(a)).

The comparison of the theoretical wave propagation characteristics calculated from the half-space models with the measured waves (i.e. the dispersion curves shown in Figure 8 or the surface plots of Figure 9 compared against measured results shown in Figure 7) can lead to the determination of the soil properties. Additional comparisons can be achieved by transforming the predicted response in the spatial domain and comparing directly the theoretical response and vibration attenuation with the measured ones. Figure 10 shows such a comparison between the receptance 24 m from the load (Figure 10(a)) and the attenuation of the vibration with distance at 31.5 Hz (Figure 10(b)) measured at the site shown in Figure 7 with the response calculated from the example model.
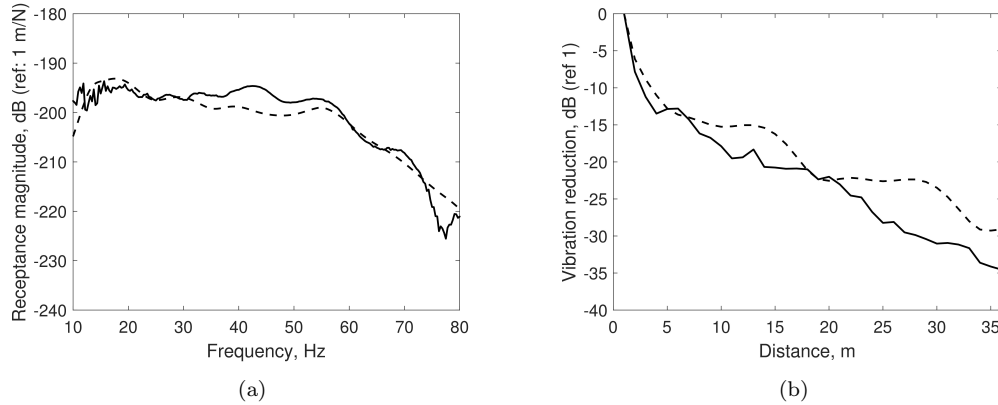

Figure 10. (a) Comparison between (———) measured and (– – –) predicted ground response: (a) receptance magnitude 24 m from the track and (b) attenuation with distance at 31.5 Hz.

For the case presented here, the geometrical (layering) and the material parameters used for the half-space model seem to have been selected appropriately in order to predict a response that agrees reasonably well with the measured response from the actual site. Such inverse problem techniques of identifying the properties of a ground model by fitting its dynamic response to that of an actual site, are the basis of the *in situ* methods for identifying the dynamic soil properties for a railway site and establishing a ground model that can be coupled to the railway model and predict ground-borne vibration [46, 53–58].

Alternatively, the dynamic soil properties can be determined using laboratory methods. The resonant column test [59] or the torsional shear test [42, 60] are often used to determine the properties of soils, but there is always risk of sample disturbance [54]. In situ tests preserve the natural condition of the soil and avoid sample disturbance. Moreover, a larger volume of the soil is tested, avoiding bias

in the results due to local variations of the soil properties.

3.2. *Wave field generated by moving loads*

Up to now, the load on the ground was considered at a fixed position and thus it only generates a time-varying response when its amplitude is also time-varying. For the case of a moving point load, even when the load amplitude is constant in time, the motion of the load will lead to a time-varying response at a fixed point. This response depends on the magnitude of the load speed relative to the wave speeds in the soil.

Figure 11 shows the predicted wave field generated by a point load of constant unit amplitude for three load speeds: v = 80 m/s, v = 168 m/s and v = 250 m/s moving on the surface of the layered half-space model presented in Section 3.1 and Figures 8-9. Figure 11(a) shows the wave field generated by the load moving at a speed which is below the wave phase velocities of the surface waves. The displacement "bowl" under the load is indicated by the positive (upward) displacement under the load. No propagating waves are generated by the moving load in this case and an observer at a fixed position in the free field will observe a time varying response with the deflection shape travelling with the load speed. When the load speed is close to the Rayleigh wave speed of the upper layer, in Figure 11(b), the wave field generated changes and the displacement amplitudes are significantly larger. The displacement is observable at greater distances along the track than for the lower speed of load and a small "bow wave" can be seen at the load position. The effects of a further increase of speed to 250 m/s are shown in Figure 11(c). At this speed, in excess of the P-SV wave speed of the layer material, a number of waves are created in the track behind the load and propagating waves may be seen travelling with significant amplitude away from the load. These create propagating waves in a "Mach cone" behind the moving load. The maximum displacement amplitudes in this case are lower than for the case of load speed equal to the Rayleigh wave speed shown in Figure 11(b).

While a moving load with a constant amplitude only generates propagating waves at load speeds close to or above the P-SV wave speeds of the soil, a moving load with a time-varying amplitude will generate propagating waves, irrespective of the load speed [61]. Moreover, for the case of a moving harmonic load, the Doppler effect occurs [62], where a load of a single frequency will produce a transient response at a fixed point in the ground which has a spectrum containing a range of frequency components. As in the case of a load with zero excitation frequency (constant amplitude), when the load speed exceeds the lowest P-SV wave velocity in the soil, the wave field displays a similar Mach cone (see Figure 11(c)), however, without the large amplification observed in the zero frequency case.

For high speed trains travelling on tracks supported by very soft soil ($c_s \leq 50$ m/s), the train speed can actually be close to or even larger than the fundamental P-SV wave speed of the ground. When this happens it may lead to a significant amplification of vibration levels and track displacements compared with the lower speed range, resulting in problems of track stability and safety. This problem of trains running at such "critical speeds" was addressed in several studies [63–66] and was confirmed by field measurements at the site of Ledsgård in Sweden where track displacements up to 10 mm were measured during the passage of the X2000 train at 200 km/h [43, 67, 68].

The critical speed at which large amplifications of track displacements are expected, is generally controlled by the P-SV wave velocities in the soil but also depends on the properties of the track [66, 69]. Figure 12 shows the maximum rail
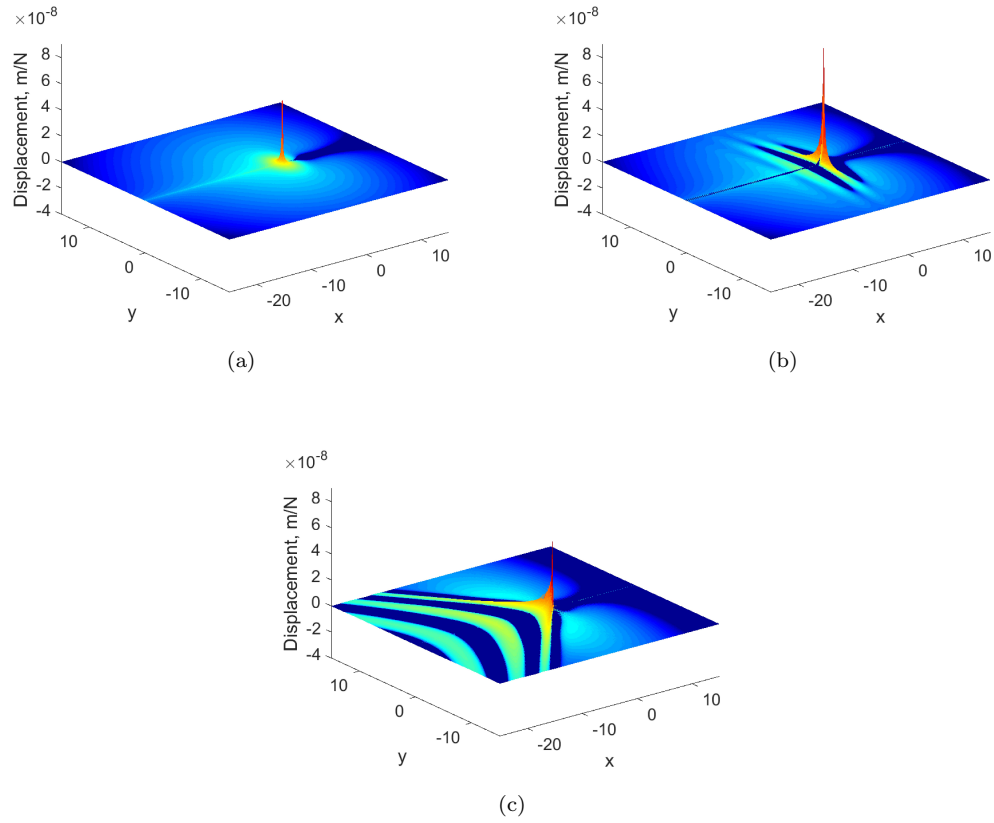
Figure 11. Displacement pattern in the moving frame of reference for a single non-oscillating point load on the ground surface moving at: (a) 80 m/s (below the wave speeds in the ground); (b) at 168 m/s, close to the Rayleigh speed of the upper layer for this ground system; (c) at 250 m/s.

response (displacement) predicted due to a unit constant load moving with different speeds on two different track forms, a typical ballasted track and a slab track, with properties given in Table 3. The results are given for a ground that has properties identical with the ground modelled in Section 3.1 except the wave speeds of the upper layer which are reduced to c_s = 90 m/s and c_p = 180 m/s. A significant increase in vibration can be seen as the load speed approaches a certain "critical" value. Comparing the rail vibration level and the values of the peak-response load speed for the two different track forms, it can be seen that for the slab track the critical speed occurs for higher speed values and the maximum rail response is lower for all speeds below the critical speed than for the ballasted track.

Since the problems encountered with high speed trains running at critical speeds are related with track stability and riding safety, they are of large concern and much effort has been given in the last decades in dealing with them. However, as they must be dealt with to alleviate these concerns, critical speed problems are not often an issue for environmental ground-borne vibration and thus they are not in the focus of the current review. In most cases apart from the choice of track type and appropriate track design, subgrade stiffening or piled track foundations can be used as mitigation measures for dealing with the critical speed problem [43, 67, 68, 70].
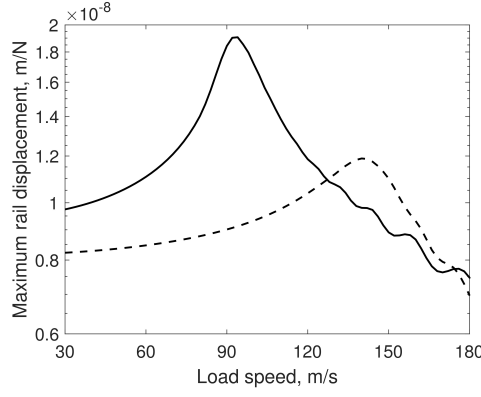
Figure 12. Maximum rail displacement with load speed for (———) ballasted track, (– – –) slab track.

Table 3. Parameters used for the ballasted track and the slab track in Figure 12.

Rail UIC60	Mass of rail per unit length	60 kg/m
	Bending stiffness of rail	6.3 MN·m^2
	Daming loss factor of the rail	0.05
Ballasted track	Rail fastening system stiffness	120 MN/m
	Rail fastening system damping loss factor	0.1
	Mass of sleepers	300 kg
	Mass of ballast per unit length of track	1740 kg/m
	Ballast stiffness per unit length of track	4640 MN/m^2
	Damping loss factor of ballast	0.2
	Sleeper spacing	0.65 m
	Ballast width in contact with ground	3 m
Slab track	Rail fastening system stiffness	50 MN/m
	Rail fastening system damping loss factor	0.1
	Rail fastening system spacing	0.65 m
	Mass of slab per unit length of track	3720 kg/m
	Bending stiffness of slab	232 MN·m^2
	Damping loss factor of slab	0.015
	Slab width	3.4 m

3.3. *Excitation mechanisms of railway ground-borne vibration*

Ground-borne vibration from railways is generated at the wheel-rail interface due to the passage of individual wheel loads along the track (quasi-static loading) and due to dynamic interaction forces caused by the interaction of the wheels and tracks (dynamic loading). When assuming a linear behaviour of the track and the supporting soil, the resulting ground vibration displacement $u(x,y,z,t)$ at a location (x,y,z) and time t can be decomposed into the quasi-static component $u_{\mathrm{qs}}(x,y,z,t)$ and the dynamic component $u_{\mathrm{dyn}}(x,y,z,t)$:

$$u(x,y,z,t) = u_{\mathrm{qs}}(x,y,z,t) + u_{\mathrm{dyn}}(x,y,z,t). \tag{16}$$

The quasi-static response can be written as a superposition of the contribution of the train axles as

$$u_{\mathrm{qs}}(x,y,z,t) = \sum_{l=1}^{N_{\mathrm{a}}} P_l u_{\mathrm{qs0}}(x - \alpha_l - vt, y, z) \tag{17}$$

where N_{a} is the number of train axles, P_l is the axle load for the l-th axle, α_l is

the position of the l-th axle and $u_{\mathrm{qs}0}(x - vt, y, z)$ is the ground response due to a unit load moving with speed v on the track along the x direction. In the frequency domain this expression can be written as [61]

$$\hat{u}_{\mathrm{qs}}(x, y, z, \omega) = \frac{1}{v}\mathrm{e}^{-i\omega\frac{x}{v}}\hat{u}_{\mathrm{qs}0}(\omega, y, z)\sum_{l=1}^{N_{\mathrm{a}}} P_l\mathrm{e}^{i\omega\frac{\alpha_l}{v}} \tag{18}$$

where now $\hat{u}_{\mathrm{qs}0}(\omega, y, z)$ is the ground response in the frequency domain due to a unit load moving with speed v on the track at $x = 0$. From the last expression it can be shown that the repeated passage of axles due to the train speed v leads to characteristic peaks and troughs in the narrow-band frequency spectrum of the response [69, 71–74]. These peaks and troughs depend on the train speed, the geometry of the train vehicle types and the separation distance of axles on a bogie. For sub-critical train speeds, the properties of such response spectra of the track can be used for rapid determination of the train speed but also for the calculation of the track system support modulus without knowledge of the axle loads [75].

Since the quasi-static loading is constant throughout the passage of the train and it only depends on the speed, the axle loads and the axle separation distances of the train, a spatially invariant model that consists only of the ground and the track is sufficient to estimate the quasi-static component of the ground-borne vibration. This is not the case for the dynamic component of the ground response. The dynamic load component is determined by the train-track interaction and results from several, more complex, excitation mechanisms. Such mechanisms are the wheel and track unevenness, the impact excitation due to wheel flats, rail joints and turnouts (switches and crossings), as well as parametric excitation due to the spatial variation of support stiffness, e.g. due to the discrete nature of sleeper or slab support or due to differential variation of the track and the subsoil. The variation in track stiffness along its length acts in a similar way to unevenness excitation. However, it has been shown [76, 77] that the excitation due to the unevenness is generally much more significant.

Hence three contributions to ground vibration are generally considered to characterize the source of vibration [78]:

(1) The moving load effect (called quasi-static contribution): it represents the response of a structure to moving vehicles where only the axle loads are considered. This effect is represented in Figure 13(a).

(2) The roughness distributed along the track and at the wheel surface: this generates a dynamic contribution where the vehicle dynamics plays a minor role and is added to the moving load effect. Full detailed modelling of the vehicle is generally not required [79].

(3) The possible localized defect(s) (rail joints or turnouts) at the wheel/rail contact (also a dynamic contribution but where the vehicle dynamics plays a greater role). Most often, such defects generate high levels of vibration and become the main contributor (Figure 13(b)). Such contributions primarily depend on the vehicle and trackbed characteristics. The wheel-rail forces mainly depend on the vehicle/track interaction [80].

In general, due to the nonlinearities of the track support components (including the soil subgrade), the vehicle suspension system and the contact mechanics, as well as due to the spatial variation of the track support and the wheel and track unevennesses, the response of the coupled train-railway-ground system is nonlinear and time-dependent. However, the models for predicting ground-borne vibration are usually developed based to some extent upon simplifying assumptions. These
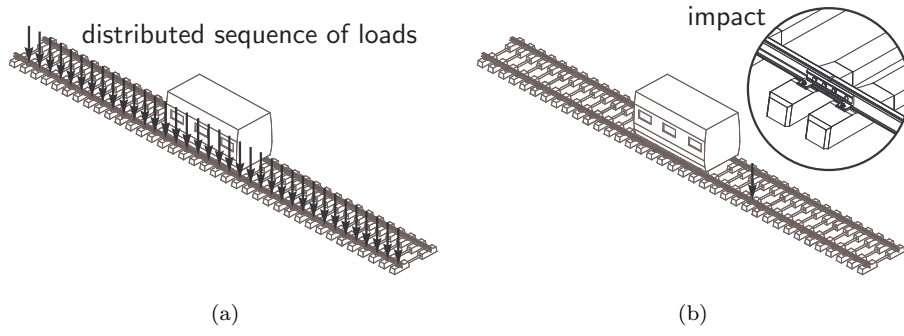
distributed sequence of loads

impact

(a)   (b)

Figure 13. Schematic representation of dynamic contributions to ground vibration: (a) for distributed source (moving load with or without roughness) and (b) for localised source of excitation

may depend on engineering insight to replicate the operational conditions of interest, or may be necessary due to a lack of complete data for the simulation, or limitations in the available computational power.

Therefore, to enable analysis in the frequency domain, apart from the assumption of a linear elastic ground that is commonly used in ground vibration problems, the track system can be assumed invariant or periodic in the longitudinal direction and any nonlinear components (i.e. rail fastening system, ballast) can be linearized, which is valid for small motion amplitudes. Similarly, for ground vibration problems the vehicle suspension can be considered as linear. Viscous or viscoelastic damping can be introduced and included in the frequency domain.

For the frequency range 1-80 Hz, typically of interest for the perception of ground vibration and 20-250 Hz for the perception of ground-borne noise, and a train speed range of 10-100 m/s (36-360 km/h), the corresponding wavelengths of the vertical unevenness lie within the range 0.04 to 100 m (or wavenumbers from 0.062 to 160 rad/m). By assuming that the wheel is always in contact with the rail, a linearized Hertzian contact spring with stiffness $k_{H,k}$ can be inserted between the k-th wheel and the rail, although for this frequency range of ground-borne vibration, inclusion of the contact spring does not influence the total response significantly and can be even ignored.

When considering the rail surface, at wavelengths less than about 1 m this vertical unevenness is most commonly caused by irregular wear or corrugation of the rail contact surface and can be measured using instruments intended for "acoustic" roughness, whereas at much longer wavelengths it is due to undulations in the track bed and should be measured using track measuring cars [58]. On the wheels, short wavelength unevenness is again caused by wear whereas discrete wavelengths up to about 3 m are present due to out-of-roundness. However, it has been shown in [81] that although the typical wheel irregularities are of a similar order of magnitude to the rail irregularities at short wavelengths (below 0.1 m; "acoustic roughness"), the magnitude of wheel irregularities is very much smaller than those of the rail at longer wavelengths and thus can be neglected for ground-borne vibration generation. Thus, all irregularities can be assumed to be on the rail surface. It has been shown in [82] that for unevenness wavelengths longer than about 3 m the unevenness of the two rails can be considered to be strongly correlated (and in phase). At shorter wavelengths the unevenness of the two rails should be considered as uncorrelated.

By assuming steady state harmonic solutions at circular frequency ω and introducing the vector $\hat{\boldsymbol{u}}_r(\omega)$ that collects the vertical rail irregularity at all contact

points the coupled track-ground system can be written as

$$[\hat{\mathbf{R}}_{\mathrm{w}}(\omega) + \hat{\mathbf{R}}_{\mathrm{r}}(\omega) + \hat{\mathbf{R}}_{\mathrm{c}}(\omega)]\hat{\boldsymbol{p}}_{\mathrm{dyn}}(\omega) = -\hat{\boldsymbol{u}}_{\mathrm{r}}(\omega) \tag{19}$$

where $\hat{\mathbf{R}}_{\mathrm{w}}(\omega)$ and $\hat{\mathbf{R}}_{\mathrm{r}}(\omega)$ are the $N_{\mathrm{w}} \times N_{\mathrm{w}}$ matrices of complex receptance (transfer function for displacement due to force) of the wheels and the rails respectively and $\hat{\mathbf{R}}_{\mathrm{c}}(\omega) = \mathrm{diag}\{1/k_{H,k}\}$ is the matrix of contact spring receptances. Eq. (19) is a set of linear algebraic equations with the dynamic wheel-rail forces $\hat{\boldsymbol{p}}_{\mathrm{dyn}}(\omega)$ as unknowns. Its solution can then be used as an input for the coupled track-ground model to give the dynamic component of the response $\hat{u}_{\mathrm{dyn}}(x,y,z,\omega)$ of the ground in the free field.

It should be noted that since the models for prediction of ground-borne vibration are usually developed by coupling sub-models for the train, the track and the ground it is possible to develop hybrid models that work in a mixed time-frequency domain. The partial use of time domain analysis allows for the consideration of nonlinear components (e.g. rail pad or ballast behaviour, Hertzian contact) as well as loss of contact between the wheel and the rail, but retain efficient calculations for an infinite linear ground medium. Examples of such models will be discussed in the next sections.

3.4. *Analytical methods*

Many different models have been developed for predicting vibration from surface and underground railways in the last few decades. As already mentioned, these models are commonly developed by coupling sub-models for the train, the track (and the tunnel for underground railways) and the ground. In general, for ground-borne noise and vibration applications much larger modelling and computational effort is required for capturing the dynamic behaviour of the track, the tunnel and the soil compared with that used for the dynamic response of the train, which is usually represented by relatively simple multibody vehicle models (Figure 14).
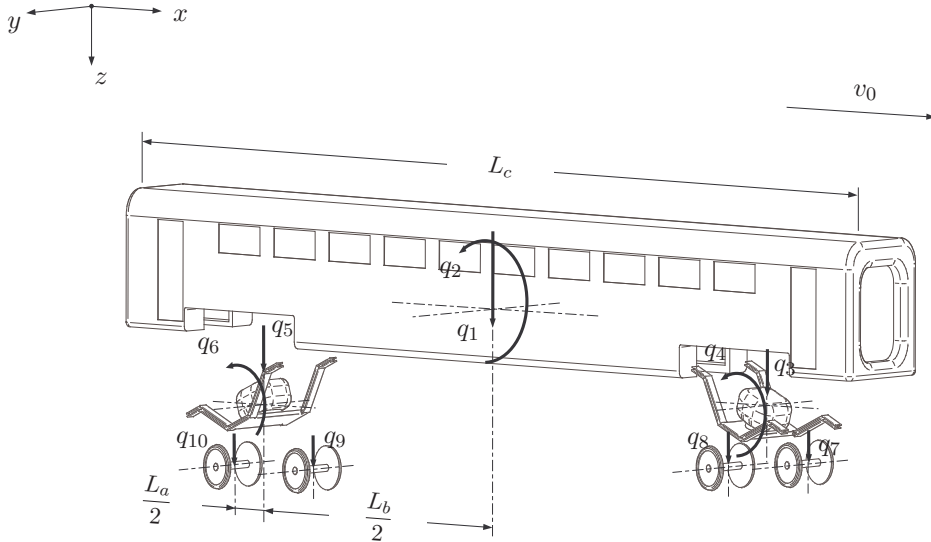

Figure 14. Vehicle modelling: usual rudimentary configuration parameters and geometry

Based on the assumption of a linear elastic medium for the soil, three-dimensional analytical models have been developed in the wavenumber-frequency domain by

using the double Fourier transformation with respect to the spatial coordinates x and y

$$\tilde{u}(k_x, k_y, z, \omega) = \int_{-\infty}^{\infty} \int_{-\infty}^{\infty} \hat{u}(x, y, z, \omega) e^{-i(k_x x + k_y y)} dx dy. \qquad (20)$$

These models assume that the track (and the tunnel where it exists) is invariant along its length and coupled to a horizontally invariant soil. The formulation leads to closed-form expressions for the prediction of the vibration in the free-field or in the body of the ground in the wavenumber-frequency domain. The three-dimensional solution $\hat{u}(x, y, z, \omega)$ is recovered by an inverse Fourier transformation with respect to the wavenumbers k_x and k_y

$$\hat{u}(x, y, z, \omega) = \frac{1}{4\pi^2} \int_{-\infty}^{\infty} \int_{-\infty}^{\infty} \tilde{u}(k_x, k_y, z, \omega) e^{i(k_x x + k_y y)} dk_x dk_y. \qquad (21)$$

A tilde and a circumflex above a variable in Eq. (20) and (21) denotes the representation in the frequency-wavenumber domain and frequency-spatial domain respectively.

For the case of railways at grade, several models were developed initially to predict only the quasi-static component of the response for a homogeneous half-space [65] or a layered half-space [67, 68, 83]. The dynamic excitation on the track was later implemented [61, 84] and this enabled the calculation of the total ground vibrational response due to the train passage [50, 72, 82, 85].

For underground railways in tunnels, a three-dimensional analytical model was first developed by Forrest and Hunt [86] for the prediction of the vibration from a tunnel buried in a full-space, where the tunnel and the soil were modelled as two concentric pipes (pipe-in-pipe or PiP model). The inner pipe, which represents the tunnel was modelled using the thin shell theory. The outer pipe with infinite radius represents the surrounding soil and was simulated by elastic continuum theory [87, 88]. The PiP model has been further improved and validated [89–91] by including a floating slab track and was used for predicting the effect of parallel twin tunnels [92] and a second deck [93]. More recently, the model has been extended to predict ground vibration from a harmonic load applied on a tunnel embedded in a multi-layered half-space [94]. However, it still uses the assumption that the tunnel is located in a full-space for the calculation of the tunnel-soil interaction forces and this deteriorates the accuracy of the model when the distance between the tunnel and the free surface or the layer interface is not larger than twice the tunnel diameter. A similar approach was proposed in [95] with the tunnel modelled an elastic hollow cylinder of finite thickness. The assumption of the full-space surrounding the tunnel is lifted in [96]; however the benchmark solutions presented are limited to cases of vibration from a point load in a tunnel embedded in a homogeneous half-space. Recently a 3D analytical model for calculation of ground vibration from a tunnel, modelled as an elastic hollow cylinder, embedded in a single layer within a multi-layered half-space was proposed in [97].

These models are considered highly computationally efficient and they are formulated using relatively modest modelling effort. This is because they are based on the closed-form solutions developed in the wavenumber-frequency domain for full-space, homogeneous half-space and the solutions derived with the flexibility matrix method [47, 48] and the dynamic stiffness method [49] for layered half-space soils. In order to obtain accurate predictions of ground-borne vibration, detailed information is needed regarding the parameters that characterize the dynamic behaviour of soil and the track as well as the excitation.

For the case of surface trains the models commonly take account of the moving load [61, 98] including the Doppler and critical speed effects, whereas for underground railways, where the train speeds are usually lower and a stiff tunnel structure is present, the assumption of a "moving roughness" can be used; the roughness is pulled through between the wheels of a fixed train and the track with the velocity of train, assuming that each wheel is excited by the same roughness apart from a time lag.

The transformation from the wavenumber domain to the spatial domain (Eq. 21) is performed numerically by an integral transform which is usually achieved using highly efficient computational algorithms such as the fast Fourier transform. This numerical implementation in the approach is the reason that this family of prediction models are known also as semi-analytical models.

The main drawback of these computationally efficient analytical models is that, due to the assumed horizontal invariance, they are not flexible to geometrical variations such as a track on an embankment or a track in an excavation (cutting). For the case of underground railways the derivations exist only for circular tunnels. Moreover, they do not allow account to be taken of discrete rail support as found in conventional ballasted or slab tracks. This implies that the stress distribution under the sleepers or the slab is not entirely correctly predicted, which is important at high frequencies when wavelengths in the track and the soil are of the same order of magnitude as the sleeper or the slab dimensions. For the same reason, they cannot account for parametric excitation, although it can be included by using an equivalent geometric unevenness [72].

3.5. *Numerical methods in the frequency domain*

To introduce the effects of more complex geometry it is necessary to use numerical approaches such as the finite element (FE) and boundary element (BE) methods. A common challenge is that the elements in the discretisation have to be small enough to represent wave phenomena: it is a usual requirement that there are at least 6 elements per wavelength [99], some authors suggesting 10 or more should be used. Consequently, as frequency increases, the number of elements increases rapidly.

When FE models are used to represent the ground, it is important that the boundaries of the finite computational domain do not introduce false reflections. The reflections from the boundaries can be minimised by adopting Infinite Elements (IE) [100–102] or Perfectly Matched Layers (PML) [103] to terminate the FE mesh.

The boundary element method includes the radiation condition implicitly. It can be used either on its own or coupled with the FE method. With the coupled FE-BE method the track and other structures such as tunnels can be modelled in detail using FE, whereas homogeneous regions of soil can be represented more efficiently by using BE. Jones et al. [104] developed a two-dimensional (2D) coupled FE-BE model and applied it to study both bored and cut-and-cover railway tunnels. It was used in [105] to study trenches adjacent to railway lines. Three-dimensional (3D) FE-BE models were compared with 2D models in [106]. It was shown that 2D models can predict correct trends but that 3D models are required to predict absolute levels. However, they involve a much higher computational cost.

Where the geometry and material properties are uniform along the direction of the track, as is usually the case, it is possible to use a so-called two-and-a-half dimensional (2.5D) approach to obtain results that include 3D effects but with significantly reduced computational time. In this approach, a 2D FE and/or BE mesh is used and the third dimension is represented by a series of wavenumbers.

The full 3D solution can be obtained by applying an inverse Fourier transform over wavenumber. Yang and Hung were among the first to use such an approach, applying it in a finite/infinite element method [100, 107–109]. Jean et al. [110] presented a 2.5D BE method for ground vibration which was later extended to include FE domains [111]. A 2.5D FE-BE model was presented by Sheng et al. [112] and applied to trains in tunnels and on an embankment [113]. A similar model was used by Jin et al. [114] to represent a metro tunnel and comparisons were made with field measurements. Coupled 2.5D FE-BE models were also applied to surface railways in [115–120]. In [121] a 2.5D model was developed based on the method of fundamental solutions coupled to the finite element method (MFS-FEM) and in [122] the finite element method was coupled with a scaled boundary finite element method (FEM-SBFEM).

In [123] a finite element model of the track (rails, rail pads and sleepers) was coupled to the soil via the Green's functions for a layered half-space using a boundary element formulation. The ballast layer was included as part of the soil. A slab track was modelled with a similar approach. In [124] the implications of the underlying soil for vehicle-track interaction are explored.

For a situation where the tunnel or track is not uniform along the third direction, Degrande et al. [125] developed a periodic FE-BE model, in which the Floquet transform was employed to represent the periodic geometry of a tunnel. However, this requires considerably more computational effort than the 2.5D approaches.

It is also possible to include buildings directly in a finite element model. For example Ropars et al. [126] considered a 3D FE model of a four-storey building on a piled foundation above a metro tunnel, requiring 1.2 million elements. However, the large size of such models means that they require very large computation times. A 2.5D approach is more efficient [111] but is restricted to long buildings that are situated parallel to the tracks. Moreover the acoustic field inside the building is incorrect as there are effectively no walls perpendicular to the tracks. To overcome this Jean developed a so-called 2.75D approach [127] which introduced a 3D modal-based model of the acoustic volumes into a 2.5D framework for the ground and building.

To include the response of buildings in the prediction models it is also possible to use a two-stage approach in which the ground response is calculated without the presence of the building and then a coupling technique is applied to determine the effect of the building on the vibration field [128, 129]. In [103] the ground response to a train in a tunnel was calculated using a 2.5D FEM-PML model of the tunnel and ground and then a 3D building model was coupled to it accounting for soil-structure interaction.

3.6. *Numerical methods in the time domain and two-stage schemes*

To take account of inhomogeneities in the track, for example a transition from a slab to a ballast track or the presence of unsupported sleepers, a full 3D model is required, usually in the time domain. Galvín et al. [130] developed a time domain fully coupled three dimensional multi-body-finite element-boundary element model to predict vibration due to train passages. The BE model used full-space Green's functions (i.e. fundamental solutions) so that the ground surface had to be meshed. Xia et al. [131] used Green's functions from a layered half-space connected beneath each sleeper in a time domain model of vehicle/track interaction.

Three-dimensional FE models solved in the time domain have been developed by Connolly et al. [102] for the response of the ground to a moving vehicle. Shih et al. also implemented a 3D FE model for critical velocity studies and included

soil nonlinearity [132, 133]. Other 3D FE models are given in [134–137]. In [138] a moving element method was introduced to reduce the model size.

To avoid the need for large FE models a two-stage hybrid approach has been introduced. Triepaischajonsak and Thompson [139] used a time domain FE model for the track coupled to a simple moving vehicle model. The soil beneath the track was represented by an equivalent spring-damper system. The forces acting on the ground beneath each sleeper were then transformed into the frequency domain and combined with analytical Green's functions for the soil to predict the response at locations away from the track. Koroma et al. [140] extended this approach to include interactions between adjacent sleepers through the ground. The response of the ground was determined by transforming the forces beneath the sleepers into the wavenumber domain so they could be applied directly in a frequency-wavenumber analytical ground model.

Nielsen et al. [141] used a similar hybrid approach combining the established time-domain vehicle/track interaction model RAVEN and the frequency-wavenumber ground vibration model TRAFFIC. In this approach the wheel/rail dynamic force was extracted from the time-domain model and used as input to the frequency-wavenumber model. This was used to determine the ground response to impact loading.

To study the ground response due to rail joints and wheel flats Kouroussis et al. [80] used a two-stage approach, in which the second stage used a full 3D FE model of the ground.

3.7. *Semi-empirical methods*

Accurate predictions of ground vibration using empirical models derived from measured data, as presented in Section 2.3, are limited to the cases where a suitable characterization of the force density and the vibration propagation is available. Recently, to overcome this limitation, empirical methods have been combined with numerical methods in semi-empirical prediction models. Such hybrid prediction models use the information obtained from measurements to improve the accuracy of numerical models, while at the same time providing the flexibility of numerical models to assess a wide range of rolling stock, track and soil parameters. Kuo et al. [142] used such a hybrid empirical-numerical methodology to assess different track arrangements and determine the effect of the installation of mitigation measures within the propagation path for the case of a railway at grade. In a similar concept, Kourousis et al. [143] presented an alternative to the FRA method [14] that can be used to assess the effect of localized rail defects and provide ground vibration predictions in the time domain.

4.   Influence of different parameters on ground vibration

In this section the influence of the main parameters of the vehicle/track system and ground vibration is reviewed.

4.1. *Vehicle parameters and wheel/rail contact*

Regarding the vehicle characteristics, one main parameter is the periodicity of the axle loads. Carbody length L_c, bogie spacing L_b and axle spacing L_a schematically describe the vehicle geometry (Figure 14). Furthermore, this rudimentary configuration allows the differentiation between twin bogies ($L_c > L_b + L_a$) and articulated

bogies ($L_c = L_b + L_a$). As it was shown in recent papers [75, 78], the shape of the ground vibration spectra primarily depends on the vehicle geometry and on the vehicle speed, combined with the deflection characteristics of the track and the ground amplification/attenuation.

To analyse vibration levels, it is first important to be able to interpret predicted vibration data. Models of the track and sequences of loads can be approximated by a number of similar events, each with individual delay times. If a moving single wheelset is considered, the wheel/rail force on the track can be mathematically represented by a Dirac function

$$f(t) = P\,\delta(t - t_k) \tag{22}$$

with P the nominal load (considered as constant), $\delta(t)$ the Dirac function and $t_k = \frac{x_k}{v}$ with x_k the time position of the impulse load. For constant speed v, Eq. (22) can be reinterpreted for both time t and distance along the track x since $x = vt$. Th corresponding Fourier transform is given by

$$F(f) = \int_{-\infty}^{+\infty} P\,\delta(t - t_k)e^{-i2\pi ft}\mathrm{d}t = P\,e^{-i2\pi ft_k} \;. \tag{23}$$

Figures 15(a) and 15(d) display both graphical representations of the Dirac function, showing the expected constant magnitude as a function of the frequency f. In reality, the wheel/rail force is not an impulse and is represented by a continuous, limited spectrum. The effect of this on the track is also frequency-limited, for which the cut-off frequency depends on the vehicle speed and the track flexibility. If two impulse loads are separated by a distance L_a (Figure 15(b)), time dependence and corresponding frequency spectrum are provided by

$$f(t) = P\left[\delta(t - t_k) + \delta(t - t_k - L_a/v)\right] \tag{24}$$

$$F(f) = P\,e^{-i2\pi ft_k}\left(1 + e^{-i2\pi f(L_a/v)}\right) \tag{25}$$

and plotted in Figures 15(b) and 15(e). An amplitude modulation is clearly observable with a beating of $f_a = \frac{v}{L_a}$ and zero amplitude at frequencies $\frac{2k+1}{2}f_a$ ($k \in \mathbb{N}$). This effect represents a single bogie force moving at speed v. For a complete carbody, a similar effect is deduced by introducing the bogie distance L_b in the time history:

$$f(t) = P\left[\delta(t - t_k) + \delta(t - t_k - L_a/v)\right.$$
$$\left. + \delta(t - t_k - L_b/v) + \delta(t - t_k - (L_a + L_b)/v)\right] \tag{26}$$

and in the corresponding Fourier transform:

$$F(f) = P\,e^{-i2\pi ft_k}\left(1 + e^{-i2\pi f(L_a/v)}\right)\left(1 + e^{-i2\pi f(L_b/v)}\right) \;. \tag{27}$$

Figure 15(f) reveals this second modulation induced by a pair of bogies: a sequence of lobes of width $f_b = \frac{v}{L_b}$ follows the envelope initially defined by Eq. (25). By generalising Eq. (27) with n_c carriages, the Fourier transform of a complete train

load function becomes

$$F(f) = P\,e^{-i2\pi f t_k}\left(1 + e^{-i2\pi f(L_a/v)}\right)$$

$$\left(1 + e^{-i2\pi f(L_b/v)}\right)\left(1 + \sum_{j=1}^{n_c} e^{-i2\pi j f(L_c/v)}\right) \qquad (28)$$

and introduces the carriage excitation frequency $f_c = \frac{L_c}{v}$ corresponding to dominant frequencies for which the spectral peaks follow the envelope [74]. A more rigorous description of the role of the vehicle geometry and the influence of bogie and axle spacing, including the number of vehicles and the variation in wheel loads, can be found in [75]. A comprehensive interpretation of the shape of a spectrum of measured track vibration is used for additional applications including, for example, the estimation of vehicle speed by analysing the ground vibration peak spectra [144].
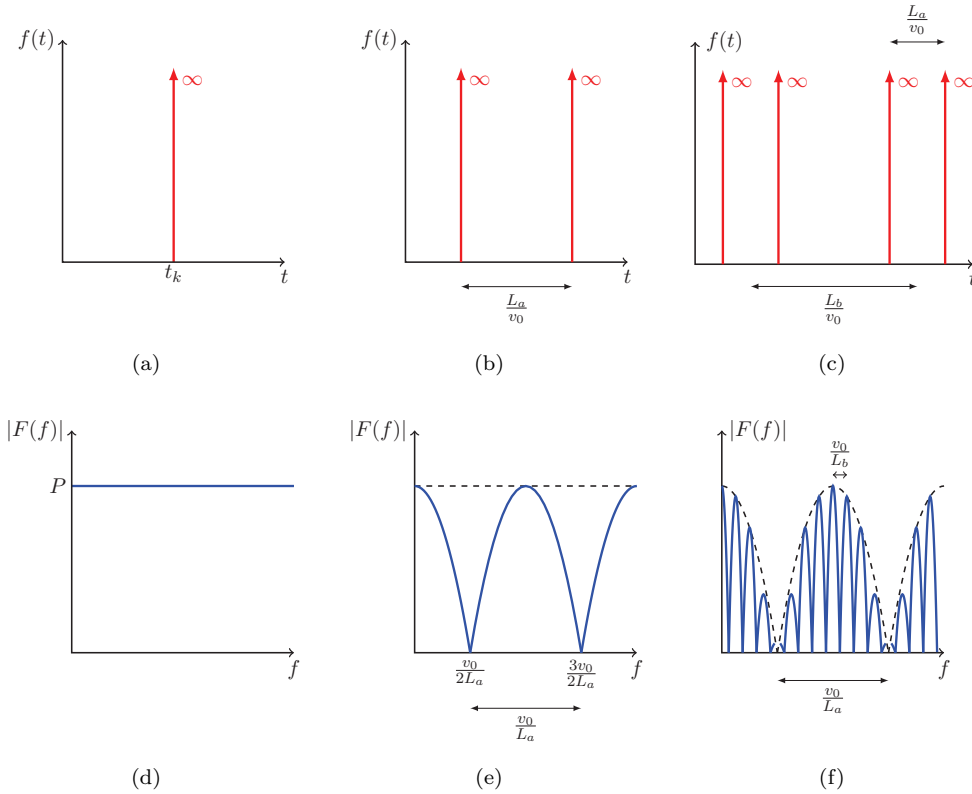

Figure 15. Carbody effect with Dirac functions: (a) single Dirac function – one wheel effect (time history), (b) double Dirac function – two wheels effect (time history), (c) quadruple Dirac function — four wheel effects (time history), (d) single Dirac function – one wheel effect (frequency content), (e) double Dirac function – two wheels effect (frequency content) and (f) quadruple Dirac function — four wheel effects (frequency content)

The aforementioned description is the basis of the periodicity observed in ground vibration spectra. It is usual to consider the track deflection $u_r(t)$ as a picture of this ground vibration for the sake of simplicity in vibration description. For instance, including a random dynamic response (due for example to the rail unevenness) in addition to the quasi-static track displacement allows the generation mechanisms to be considered separately. If the whole prediction model has a linear behaviour, such a condition can be written, similarly with Eq. (16) for the ground

response, as [78]

$$u_r(t) = u_{\mathrm{r,qs}}(t) + u_{\mathrm{r,dyn}}(t) \tag{29}$$

where $u_{\mathrm{r,qs}}(t)$ is the track deflection due to axle loads, and $u_{\mathrm{r,dyn}}(t)$ the track displacement induced by the irregular track or/and wheel surface contact. The wheel/rail force model generally used for such applications is the Hertzian contact formulation either in its original form (non-linear) or in the simplified form (linearised) [145]. The vertical dynamic forces generated by the contact and acting between each wheel i and the rail can be written as

$$F_{\mathrm{rail/wheel},i} = \begin{cases} -K_{Hz}\, d^{3/2} & \text{if } z_{\mathrm{wheel},i} > z_{\mathrm{rail}} \\ 0 & \text{otherwise} \end{cases} \tag{30}$$

$$= -F_{\mathrm{wheel},i/\mathrm{rail}} \tag{31}$$

where K_{Hz} is determined from the radii of curvature of the wheel and rail surface, and from the elastic properties of their materials. $z_{\mathrm{wheel},i}$ and z_{rail} represent the vertical positions of the wheel and of the rail, respectively. d is thus the material deformation equal to $z_{\mathrm{wheel},i} - z_{\mathrm{rail}}$. In many existing railway ground vibration models, a linear contact law is assumed for the vehicle/track coupling. Eq. (30) is therefore simplified by Δd around the nominal value d_0

$$F_{\mathrm{rail/wheel},i} = F_0 + k_{Hz}\Delta d \tag{32}$$

with

$$k_{Hz} = \left. \frac{\partial F}{\partial d}\right|_{d_0,F_0} = \frac{3F_0}{2d_0} \ . \tag{33}$$

F_0 is thus responsible for the quasi-static track deflection $u_{\mathrm{r,qs}}(t)$ and $k_{Hz}\Delta d$ for the dynamic track displacement $u_{\mathrm{r,dyn}}(t)$. Many linear models have been used for the prediction of vibration for distributed track irregularity (and for moving load problem). Recently, a few research works have included a non-linear model but without a clear justification. In [80], it was clearly demonstrated to model the wheel/rail contact using a non-linear contact algorithm when singular defects are present; a linear model fails to represent the complex interaction between the wheel and the defect (loss of contact, large force variation, . . .). In addition, track flexibility and vehicle dynamics play an important role in the force calculation. This is why a complete vehicle/track model is necessary and thus a coupling between them during the simulation. This is illustrated in Figure 16, showing a comparison between measured field results and two predicted results in the case of a tram running at relatively low speed (30 km/h) over a localised defect (rectangular geometrical shape of height 1 mm and 5 mm). Two vehicle models were considered [146]:

- a simple model composed of unsprung masses, defining the wheels, undergoing a static force representing the loads applied by the bogie, assumed to be constant (axle load type model),
- a detailed vehicle model (multibody model).

The results allow an efficient comparison with the experimental data, and show the poor agreement with the results yielded by the simple model in such a situation.

Apart from the direct effect in the quasi-static vibration component that can be achieved by reducing the axle loads, modifications in the dynamic properties of the
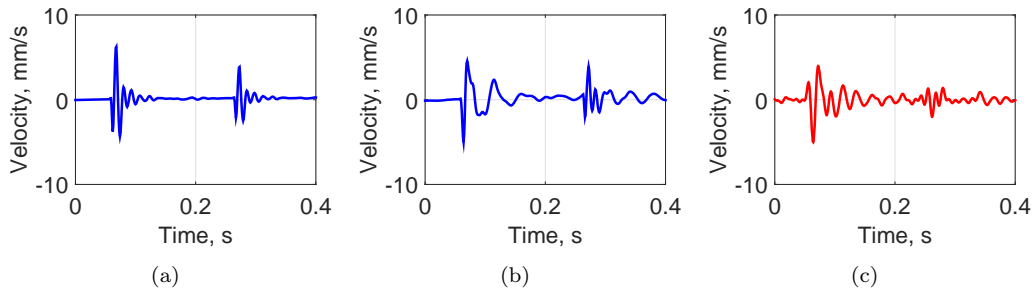
Figure 16. Time histories of vibration velocity at $2\,\mathrm{m}$ from the track for a T2000 tram — first bogie effect — running at $30\,\mathrm{km/h}$ over a localised defect [146]: (a) from a simple vehicle model (loaded wheelset), (b) from a detailed vehicle model (multibody modelling) and (c) field measured

train system can also lead to reduction of the ground vibration. Measurements of ground vibration at sub-critical speeds in [147] showed vibration levels increasing with speed. Also, the effect of the vehicle parameters on railway-induced ground vibration was studied and showed that the parameters of most influence are the unsprung mass and the stiffness of the primary suspension, with higher vibration levels occurring for heavier unsprung masses and for stiffer primary suspensions. However, for the range of vehicle parameters investigated, the effect on the levels of ground-borne vibration are relatively small.

Similar findings are shown in Figure 17 where the reduction in ground-borne vibration at 16 m from the track due to a reduction of the unsprung mass, the bogie mass and the primary suspension stiffness is given as a level difference in dB relative to a nominal train model. The results for this example are given in one-third octave bands using the model presented in [82] and the train parameters for the nominal model given in Table 4 (also given in [148] but for the results in Figure 17 a four vehicle train model was used).
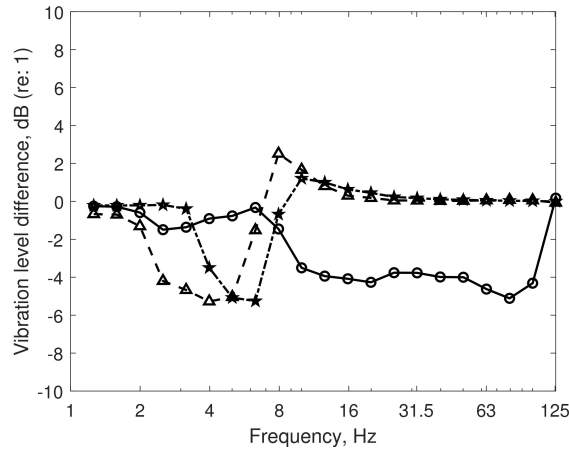

Figure 17. One-third octave spectra of the ground vibration level difference 16 m from the track between the nominal train model (Table 4) and the model with (o) 1200 kg wheelset mass, ($\triangle$) 2500 kg bogie mass and ($\star$) 1200 kN/m primary suspension stiffness

It can be seen that by reducing the unsprung mass from 1800 kg to 1200 kg per wheelset the levels of ground-borne vibration are reduced for the whole range of feelable vibration (between 2 Hz and 80 Hz) with a maximum reduction of 5 dB at the 80 Hz one-third octave band. However, above 125 Hz, in the frequency range of ground-borne noise, the reduction of the unsprung mass could lead to an increase of vibration in the ground. The modifications of reducing the bogie mass from

Table 4. Vehicle parameters for nominal train.

Car body	Mass	m_c = 40000 kg
	Pitching moment of inertia	$J_c = 2 \cdot 10^6$ kg·m^2
	Overall vehicle length	l_v = 26.6 m
Bogie	Mass	m_b = 5000 kg
	Pitching moment of inertia	J_b = 6000 kg·m^2
	Half distance between bogies	l_b = 9.5 m
Wheelset	Mass	m_w = 1800 kg
	Total axle load	P = 140.3 kN
	Contact stiffness (per wheel)	k_H = 1.2 GN/m
	Half distance between axles	l_w = 1.35 m
Primary suspension	Vertical stiffness per axle	k_{p1} = 2400 kN/m
	Vertical viscous damping per axle	c_p = 30 kN·s/m
Secondary suspension	Vertical stiffness per axle	k_{s1} = 600 kN/m
	Vertical viscous damping per axle	c_s = 20 kN·s/m

5000 kg to 2500 kg and reducing the primary suspension stiffness from 2400 kN/m to 1200 kN/m can also lead to a further small reduction of the ground vibration between 2 Hz and 6 Hz, but above 10 Hz these changes lead to small increases in vibration level.

Another important parameter that affects the ground vibration level is the vehicle speed. From the beginning, the scientific community generally agreed that increasing vehicle speed leads to increase in ground vibration. This was motivated by the so-called supercritical phenomenon. When the vehicle speed is close to (or greater than) the critical velocity of the soil (Rayleigh wave speed), the moving load problem becomes dominant (see Section 3.2). However, although track displacements typically increase with train speed, this is not always true for ground-borne vibration. For example, the converse has been found in [149–151]. The effect is mainly due to the vehicle dynamics and the particular vehicle modes that contribute to the vehicle/track interaction forces during the passing over a singular defect.

4.2. *Track parameters*

A large amount of track designs, and therefore of track parameters, can be considered. Track can be primarily classified into ballasted and non-ballasted designs. Comparison of vibration performance of slab and ballasted track designs has a practical sense if other track elements are identical. However, each of these elements is usually chosen for a specific configuration. Using a model to analyse the influence of some typical railway track parameters on the level of ground vibration induced in the neighbourhood is straightforward: it was established [152] that stiffness variation of track elements has a large influence on ground vibration levels, with other parameters having a smaller influence, namely the mass of those track elements or the sleeper spacing (Figure 18).

The support condition was treated by Metrikine et al., demonstrating that a continuously supported rail [153] or one periodically supported by the sleepers [154] provide a similar vertical deflection of the rail. The vibration performance of ballasted track and of slab track have been shown to be very similar if an equivalent railpad stiffness is used [155].

Track stiffness is the key parameter in ground vibration [156]: if it is too high, then the wheel loads are concentrated within a small area under the rail thus generating high levels of vibration, in addition to other undesirable effects (such
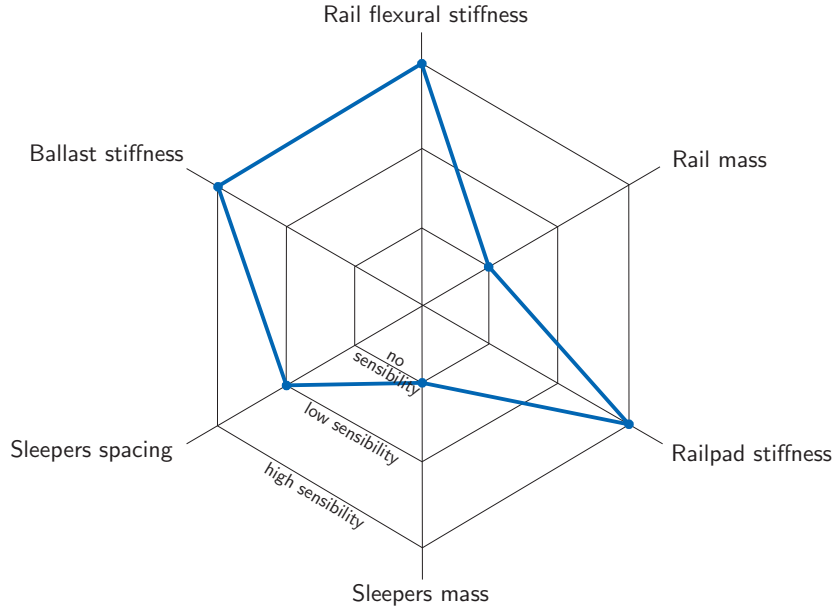
Figure 18. Sensitivity analysis summary for track parameters on ground vibration level (information issued from [152])

as corrugation).

In addition flexible track elements introduce isolation, preventing vibration from being transmitted to the neighbourhood. The principle of vibration isolation through the track stiffness is illustrated in Figure 19 using a simple single degree of freedom system. The ratio of the amplitude of the force transmitted to the foundation to that of the oscillatory force applied to the mass is called transmissibility. At very low frequency this ratio is unity; the whole force is transmitted as it would be in the static case. At the natural frequency of the system f_n, the force is increased. Above $\sqrt{2}$ times the natural frequency, the transmissibility reduces to below unity and continues to decrease with increasing frequency. Here a hysteretic damping model has been used (constant damping loss factor) that reflects the behaviour of elastomeric materials. The effect of the damping in the support and reducing the support stiffness is also shown in Figure 19. The effect of this in terms of track design is discussed in Section 5.2.

Trackbed configuration is also an important parameter. In [157, 158], it was observed that vibration energy can be trapped within an embankment, especially if the underlying soil and embankment materials have different stiffness properties.

4.3. *Ground parameters*

In practice, the ground is considered as linear, with non-linear behaviour of the soil being often neglected considering the low shear strain values. Soil stiffness — Young's modulus or shear modulus — affects the level of ground vibration as well as the attenuation with distance [159]. The effects are more complicated for heterogeneous soil for which the dispersion curves can provide more information by analysing the modes of vibration in the ground (see Section 3.1) [50, 69]. Soil damping also affects the attenuation of ground vibration as a function of the distance from the source, especially at higher frequencies.

Ground motion amplitude also depends on soil stratification, including the layer thickness, and on the frequency content of the soil surface load [160]: at greater distances from the track, the layering plays an important role. For example, the
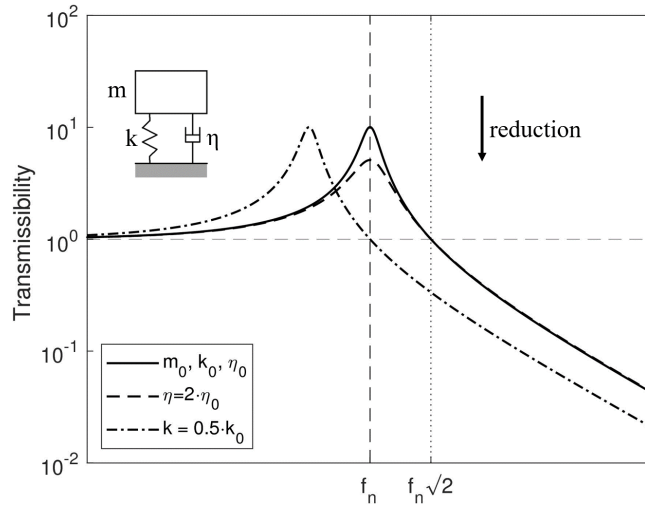
Figure 19. The force transmissibility of (———) a hysteretically damped single degree of freedom system; (− − −) for increased damping loss factor; (− · −) for reducing the spring stiffness.

attenuation of ground vibration, often associated to a power–law of the form d^{-q}, depends on the soil configuration with a large variation of the parameter q (between 0.5 and 1.1 for railway traffic [161]). Summarizing the influence of ground parameters in a few sentences is not an easy task. Regarding the study of topography effects, a large amount of research has been performed in the field of seismic wave propagation showing intense amplification or attenuation due to local geometric conditions. The soil is also rarely considered as a half-space and human activities have locally modified its composition due to local construction, especially in urban conditions.

For soft soil, a strong coupling exists between the soil and the track, and a resonance-like phenomenon occurs in high-speed cases [162]. Non-linearity should then not be neglected in prediction models. Recently, Shih et al. [132] studied different situations and showed that a non-linear model gives better results for high speeds, above 70% of the critical speed.

5. Mitigation measures for ground vibration and ground-borne noise

5.1. *Mitigation of feelable vibration*

Considerable efforts have been made in order to reduce the generated vibration, by designing mitigation solutions, but some specific locations need an intensive vibration assessment. During the last decade, a large amount of research has been done to evaluate the impact of railway lines on neighbouring structures. The purpose of this section is not to be exhaustive but to present the relevant mitigation measures proposed by the industrial and scientific communities, without omitting the limitation of these solutions. It is suggested to classify mitigation solutions as actions on the source (vehicle-track interaction), on the transmission path (track and ground), or on the receiver (building).

Mitigation measures can first be proposed for the track and the soil. Trenches and isolating screens were firstly suggested to isolate railway-induced vibration at high frequencies [120, 163–165]. The required depth is calculated in terms of the Rayleigh wavelength: a trench or a barrier is therefore invisible for long wavelength or low frequency vibration. However, if the ground has a soft layer above a stiffer

ground, a trench or soft barrier that cuts through the top layer can be particularly efficient [120]. The effect of the length is important although the width has little effect on screening vibration [164]. A barrier with a soft fill material is much less effective than an open trench but still has some potential benefit. It is the stiffness of the barrier material and not its impedance that is the most important material parameter [120]. The efficiency of stiff barriers close to a track depends on the stiffness contrast between the soil and the stiffening material and they can form a wave impeding barrier above a critical frequency [166]. Stiffening the ground beneath the track can also yield some reduction in vibration [167]. Another mitigation measure considered recently is the placing of heavy masses on the ground surface beside the track [119]. These attenuate the vibration propagation especially around the resonance frequency of the mass bouncing on the ground stiffness. A detailed review of such reflectors, including the physical mechanisms, the practical construction and the modelling parameters, can be found in [168]. The building type can also affect the transmission path [169, 170]. Base isolation techniques can be adopted as passive vibration mitigation systems in buildings [169, 171, 172].

For low frequency feelable vibration it is difficult to introduce vibration isolating technology. The most important parameter for low frequency vibration that can be influenced in the track is the vertical alignment. For ballasted track this can be improved for example by tamping to reduce the unevenness and therefore the excitation of vibration. Slab tracks have the potential to be constructed with a lower initial unevenness if the correct tolerances are applied during construction [82]. A detailed evaluation of mitigation methods dedicated to the trackbed was recently conducted in [173], with the aim of life-cycle performance analysis. Transition zones can be analysed to avoid abrupt changes in the track's vertical stiffness [174, 175]. Rail suspension fasteners attenuated the dynamic interaction between the track and the vehicle in some specific frequencies [176]. Floating slab solutions were often adopted as efficient mitigation measures (e.g. [177, 178]) but can present a negative effect for feelable vibration by increasing the track response at low and medium frequencies: the principles of base isolation can explain this phenomenon (by reference to a single-degree-of-freedom model where the track is represented by a mass and the floating slab as a spring-damper element, see Figure 19). A second stage of mitigation solution can be proposed by means of dynamic vibration absorbers which reduce the amplification induced by a floating slab [179]. This was successfully applied to underground lines [180]. For both solutions, material damping of constitutive elements is of great importance and needs to be optimized (not too high, not too low). Other applications of dynamic vibration absorbers are found for railway bridge vibration [181].

Redesigning localized defects is also considered as an efficient mitigation measure. As for noise reduction, actions at the source, when workable, are more efficient. A method to optimise the design of railway turnouts was proposed in [182] by studying the effect of the stiffness variations on dynamic train/turnout interaction. A similar research work was proposed by Bruni et al. [183] based on a vehicle/track model only. Other example can be found for permanently dipped rail joints [184], multiple wheel flats [185], wheel polygonisation [147], rail joints [186] or lift-over crossings [187].

Actions on the vehicle are more scarce but are also effective. Corrective maintenance of some vehicle elements influencing the dynamic wheel/rail contact loads and inducing ground-borne vibration remains an important measure [188]. The key of such measures is often based in reducing the unsprung mass (Figure 17). In a similar way, including resilient material in the wheel or adapting this resilience to be softer has a significant effect in the reduction of transmitted wheel/rail forces

and consequently of the perceived vibration level (up to 70% [149]). By redesigning the vehicle, it is possible to obtain a significant amplitude reduction. For example, dynamic vibration absorbers dedicated to a bogie and well tuned provide an interesting solution to mitigate excessive levels of vibration in urban areas [189].

5.2. *Mitigation of ground-borne noise*

In common with feelable vibration, ground-borne noise can be controlled at different levels at the source (train-track-soil interaction), in the transmission path, or at the receiver. Sometimes, for example with a new building near an existing railway, it is necessary to introduce base isolation within the building itself [172]. This is especially necessary in sensitive spaces such as concert halls and theatres. In the present discussion, mitigation measures in the transmission path such as vibration screening and at the receiver (building) such as base isolation of buildings or box-in-box arrangement of rooms will not be considered further. The focus is placed on the dominant mechanism of vibration excitation and of interaction between the track and the ground.

The main way in which the ground-borne noise is controlled, is using soft or "resilient" elements in the vertical support of the track in order to provide some degree of vibration isolation. From the force transmissibility curves shown in Figure 19 it can be seen that the amplitude at the resonance is dependent on the damping in the support but the degree of vibration isolation at higher frequencies is not (for this hysteretic damping model). When reducing the support stiffness, the natural frequency of the system is reduced and a greater degree of vibration isolation is achieved at higher frequencies.

Vibration isolating tracks are commonplace in modern underground railway systems to reduce ground-borne noise and the subject is an important part of track design [190]. They can also be used for surface railways; however, the insertion loss achieved will be less than for a track in tunnel unless a high impedance foundation, for example a concrete raft, is introduced beneath the track. These track forms work on a principle similar to that shown in Figure 19. In order to isolate the track dynamically, resilient elements can be included at different levels in the track structure. The lower the stiffness of the support is, the lower the natural frequency of the system will be and the greater the degree of vibration isolation at higher frequencies. The choice of support stiffness is, however, limited by the allowable vertical and lateral static displacements under the axle loads of the train.

Figure 20 shows some of the basic track design concepts for ground-borne noise mitigation. In Figure 19 and in the discussion below the rail pad is not addressed; it generally has a stiffness higher than that of the resilient element in each case but possibly still significant in the behaviour of the track design for the relevant frequency range. Moreover, the geometric track unevenness is assumed as the main source of vibration generation mechanism. Adding resilience in the track system may also lead to smoothening of the variations in the support stiffness such as parametric variation (due to sleeper passing or slab length) and variation in ballast or subgrade properties. In this way, the resilient track systems may lead to a reduction of vibration at relatively low frequencies [191]. An important reduction in perceived unevenness may also occur when the unevenness source is located beneath the resilient element, whereas an increase is possible otherwise [192].

The ballast layer forms a resilient component for a conventional ballasted track. For this reason, ballastless tracks (slab tracks) with normal pad stiffness give rise to increased vibration transmission compared with ballasted track. Designs of soft fastening systems are used to rectify this. There are many designs of soft fastening
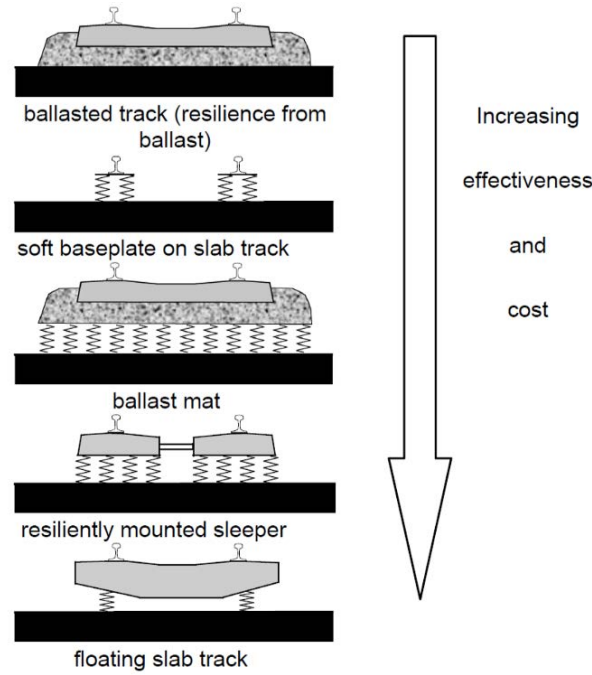
Figure 20. Design concepts for vibration isolating tracks

systems, with the standard test loadings for rails generally the limiting factor to which the vertical stiffness of the system can be lowered. In order to avoid rail rotation and consequent gauge widening, particularly during curving, such designs of baseplate are wide, or support the rail under the head.

The most common designs of soft fastening systems are the soft baseplate systems. Baseplates allow the rail support stiffness to be reduced to about 12 MN/m per fastener. They are mostly used on slab track but can also be installed on top of sleepers in ballasted track. A typical soft baseplate design is the two-stage baseplate system. It consist of a relatively stiff rail pad between the rail and a metal plate, beneath which a thicker soft elastomeric pad is used. Some baseplates also have isolated bolts through to the foundation. These must allow for movement under the trainload deflection to avoid short-circuiting the resilience of the lower elastomeric pad.

There are also different systems available for achieving a low vertical stiffness and at the same time limiting the lateral displacement of the railhead. There are systems that can achieve vertical stiffness under 10 MN/m per fastener; however, an undesirable effect of such low resilience systems is that they may lead to an increase in rolling noise. This is because the soft support leads to lower track decay rates [145]. There have been also reports that they can lead to corrugation of the rail due to the increase of the rail vibration at low frequencies.

As an example of the effect of reducing the fastening stiffness, Figure 21, shows the level difference in ground-borne vibration at 16 m from the track due to reduction of the rail fastening stiffness. The level difference is given in dB relative to a nominal surface railway model presented in [82] using a railpad stiffness of 350 MN/m and the parameters given in Tables 3 and 4. The values of the stiffness used for the comparison are selected to represent a soft railpad standard-clip case (120 MN/m), a standard baseplate system case (30 MN/m), a soft two-stage baseplate system (12 MN/m) and a very soft fastening system with 9 MN/m. It can be seen that the level difference is positive in the range of feelable vibrations (below 80 Hz) with the reduction of the fastening stiffness corresponding to an increase in

maximum ground vibration levels. For higher frequencies, vibration reduction is predicted, which should be largest (as shown in Figure 19) at the axle-track resonance frequency before the installation of the resilient rail support. Consequently, resilient track forms are generally not used for feelable vibration but are a common solution for ground-borne noise.
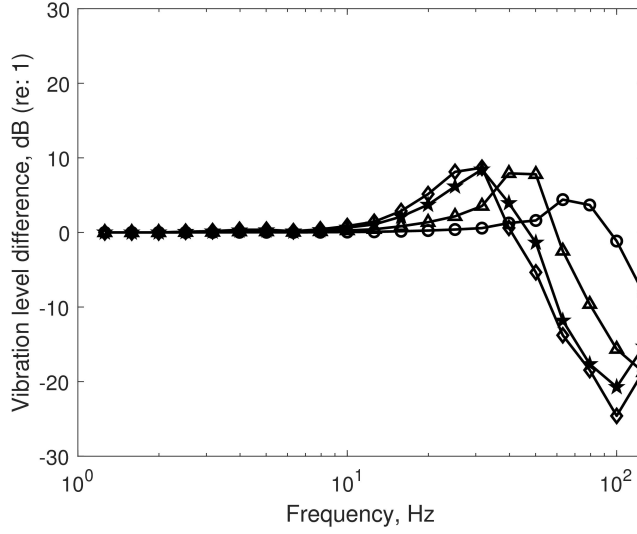

Figure 21. Ground vibration level difference in one-third octave bands; due to reductions of the rail fastening system stiffness between the nominal track model (Table 3) with 350 MN/m and the model with: (o) 120 MN/m; (△) 30 MN/m; (☆) 12 MN/m;; (◇) 9 MN/m.

Under-sleeper pads and ballast mats can be used for ballasted tracks and they lower the stiffness of the ballast layer and therefore the track resonance frequency [191, 193–196]. Booted sleepers perform in the same way as under-sleeper pads but they are used on slab tracks [190]. Since for all these cases the soft material is installed below the sleeper, the sleeper mass helps to lower the coupled wheel/track resonance frequency.

Under-sleeper pads have the advantage that they are easy to install during a sleeper renewal operation, since they are delivered already fixed to the bottom of the sleeper [197]. Ballast mats can be laid on tunnel inverts or a prepared subgrade and have the additional advantage that the extra mass of the ballast is above the spring in the resonant system. However, if a ballast mat is too soft there is a risk of making the ballast layer unstable under the vibration of passing trains and therefore compromising ride quality and increasing maintenance costs [195]. For the case of the booted sleepers, these are usually bi-block sleepers and their design and installation is integrated with the slab track.

Floating-slab tracks are used to control vibration and ground-borne noise from underground trains where a large reduction is required [198]. The track is mounted on a thick concrete slab that rests on rubber bearings, glass fibre, or steel springs. With such designs, the highest possible mass is added above the track spring to form a system with a very low resonance frequency.

Floating-slab tracks are typically designed as part of the tunnel structure. As well as the greater construction cost of the track form itself, great expense can come from any increase in the diameter of the tunnel that has to be made to accommodate sufficient mass for the floating slab. The slab may be cast in situ, resulting in a continuous length of concrete, or may be constructed in discrete precast sections laid end to end. The continuous slab designs usually have a lower deflection for a given resonance frequency and make maximum use of the tunnel

space but have the disadvantage that they are harder to design in such a way that the slab mounts can be replaced.

6. Open questions and areas for future research

With the development of ever more powerful computers, it is becoming possible to implement larger and larger numerical models, making it feasible in principle to study more complex geometries, including soil inhomogeneities and nonlinearity and even to include buildings directly in the same model. However, these models require accurate input data, which particularly for the soil properties and geometry are very difficult to obtain. The usefulness of such large models is therefore much more limited than it might appear. Despite such advances in modelling techniques, it remains the case that relatively large prediction uncertainties remain; as posed in [199] the question remains whether it is possible to achieve an accuracy better than ±10 dB.

Hand in hand with model development, improved methods for determining ground properties in situ are clearly required. The development of hybrid experimental/computational methods is promising as this can eliminate some of the sources of uncertainty. In addition there remains a role for simpler models for use in scoping studies [200, 201] and in studying parametric dependencies or determining correction factors. Other recent developments including two-stage time domain/frequency domain methods discussed in Section 3.6 are also promising.

For the mitigation of ground vibration, vibration isolation at the track or the building has long been considered for higher frequency vibration. Mitigation of lower frequency vibration remains problematic. The potential for resilient track forms to reduce the perceived unevenness [192] requires further verification in practice. Practical tests are required to verify the performance of novel mitigation measures such as heavy masses on the ground surface or wave barriers. There is also interest in the use of meta-materials, for example using arrays of inclusions in the soil to attenuate particular bands of frequency [202]. In terms of vehicle design the introduction of designs intended to reduce track forces, particularly through reduced unsprung mass, is directly beneficial to ground vibration.

Further work is needed to study the combined annoyance from noise and vibration. An initial attempt was proposed in [203] based on a common framework for the assessment of annoyance from both noise and vibration. In addition laboratory studies are required to investigate inter-dependencies.

There is a need for harmonisation of metrics used to assess whole-body vibration and for the introduction of common criteria in a similar way to that introduced in the EU for airborne noise. However, the ideal of a common calculation method appears to be extremely challenging due to the complexities and variabilities of the problem. Whereas noise maps have been introduced for airborne noise, the equivalent for ground vibration and ground-borne noise would involve the added complication of the transmission into the building itself.

versity of Southampton repository at `https://doi.org/10.5258/SOTON/D0842`.

References

[1] EC Transport White Paper: Roadmap to a single European transport area towards a competitive and resource efficient transport system, March 2011. COM(2011).

[2] Directive 2002/49/EC of the European Parliament and of the Council of 25 June 2002 relating to the assessment and management of environmental noise. *Official Journal of the European Communities*, L189:12–25, 2002.

[3] P. de Vos. Railway induced vibration: state-of-the-art report, UIC International Union of Railways, 2017. Paris.

[4] M. J. Griffin. *Handbook of human vibration*. Academic Press, London (UK), 1990.

[5] International Organization for Standardization. *ISO 2631-1: Mechanical vibration and shock – Evaluation of human exposure to whole-body vibration – Part 1: General requirements*, 1997.

[6] International Organization for Standardization. *ISO 2631-2: Mechanical vibration and shock — Evaluation of human exposure to whole-body vibration — Part 2: Vibration in buildings (1 to 80 Hz)*, 2003.

[7] British Standard. *BS 6841: Measurement and evaluation of human exposure to whole-body mechanical vibration and repeated shock*, 1987.

[8] British Standard. *BS 6472-1: Measurement and evaluation of human exposure to whole-body mechanical vibration and repeated shock*, 2008.

[9] International Organization for Standardization. *ISO 4866: Mechanical vibration and shock — Vibration of fixed structures — Guidelines for the measurement of vibrations and evaluation of their effects on structures*, 2010.

[10] Deutsches Institut für Normung. *DIN 4150-2: Structural vibrations — Part 2: Human exposure to vibration in buildings*, 1999.

[11] Deutsches Institut für Normung. *DIN 4150-3: Structural vibrations — Part 3: Effects of vibration on structures*, 1999.

[12] Association Suisse de Normalisation. *SN-640312a: Les ébranlements — Effet des ébranlements sur les constructions*, 1992.

[13] Standards Norway. *NS 8176: Vibration and shock — Measurement of vibration in buildings from landbased transport and guidance to evaluation of effects on human beings*, 2005.

[14] C. E. Hanson, J. C. Ross, and D.A. Towers. *High-Speed Ground Transportation Noise and Vibration Impact Assessment*, 2012. Federal Railroad Administration, DOT/FRA/ORD-12/15.

[15] C. E. Hanson, D. A. Towers, and L. D. Meister. *Transit Noise and Vibration Impact Assessment*, 2006. Federal Transit Administration, FTA-VA-90-1003-06.

[16] International Organization for Standardization. *ISO 14837-1: Vibrations mécaniques — Vibrations et bruits initiés au sol dus à des lignes ferroviaires – Partie 1 : Directives générales*, 2005.

[17] R. Taiar, C. Bittencourt Machado, X. Chiementin, and M. Bernardo-Filho, editors. *Whole Body Vibrations: Physical and Biological Effects on the Human Body*. CRC Press, 2018.

[18] G. Kouroussis, C. Conti, and O. Verlinden. Building vibrations induced by human activities: a benchmark of existing standards. *Mechanics & Industry*, 15(5):345–353, 2014.

[19] D. Ainalis, L. Ducarne, O. Kaufmann, J.-P. Tshibangu, O. Verlinden, and

G. Kouroussis. Improved analysis of ground vibrations produced by man-made sources. *Science of the Total Environment*, 616-617:517–530, 2018.

[20] K. Shin and J.K. Hammond. *Fundamentals of Signal Processing for Sound and Vibration Engineers*. Wiley, Chichester, 2008.

[21] G. Kouroussis, J. Florentin, and O. Verlinden. Ground vibrations induced by intercity/interregion trains: A numerical prediction based on the multibody/finite element modeling approach. *Journal of Vibration and Control*, 22(20):4192–4210, 2016.

[22] D. Waddington, J. Woodcock, M. G. Smith, S. Janssen, and K. P. Waye. Cargovibes: human response to vibration due to freight rail traffic. *International Journal of Rail Transportation*, 3(4):233–248, 2015.

[23] P. Elias and M. Villot. Review of existing standards, regulations and guidelines as well as laboratory and field studies concerning human exposure to vibration. Technical report, RIVAS project SCP0-GA-2010-265754, Deliverable D1.4, Report to the EC, October 2011.

[24] International Organization for Standardization. *ISO 14837-31: Mechanical vibration Ground-borne noise and vibration arising from rail systems. Part 31: Guidelines on field measurements for the evaluation of human exposure in buildings*, 2017.

[25] S. Yokoshima and A. Tamura. Combined annoyance due to the shinkansen railway noise and vibration. In *International Congress on Noise Control Engineering 2005, INTERNOISE 2005*, volume 1, pages 806–813, 2005.

[26] P. Jik Lee and M. J. Griffin. Combined effect of noise and vibration produced by high-speed trains on annoyance in buildings. *Journal of the Acoustical Society of America*, 133(4):2126–2135, 2013.

[27] D. P. Connolly, G. P. Marecki, G. Kouroussis, I. Thalassinakis, and P. K. Woodward. The growth of railway ground vibration problems a review. *Science of the Total Environment*, 568:1276–1282, 2016.

[28] J. De Avillez. *Routine procedures for the assessment of rail vibration*. EngD Thesis, Loughborough University, 2013.

[29] E. C. Bovey. Development of an impact method to determine the vibration transfer characteristics of railway installations. *Journal of Sound and Vibration*, 87(2):357–370, 1983.

[30] J. Nelson and H. Saurenman. Prediction procedure for rail transportation groundborne noise and vibration. *Transportation Research Record*, 1143:26–35, 1987.

[31] H. Verbraken, G. Lombaert, and G. Degrande. Verification of an empirical prediction method for railway induced vibrations by means of numerical simulations. *Journal of Sound and Vibration*, 330(8):1692–1703, 2011.

[32] K. A. Kuo, G. Lombaert, and G. Degrande. Quantifying dynamic soil-structure interaction for railway induced vibrations. In *Procedia Engineering*, volume 199, pages 2372–2377, 2017.

[33] K. A. Kuo, G. Lombaert, and G. Degrande. Quantifying uncertainties in measurements of railway vibration. In *Notes on Numerical Fluid Mechanics and Multidisciplinary Design*, volume 139, 2018.

[34] J. Sadeghi, M. H. Esmaeili, and M. Akbari. Reliability of FTA general vibration assessment model in prediction of subway induced ground borne vibrations. *Soil Dynamics and Earthquake Engineering*, 117, 2019.

[35] K. A. Kuo, M. Papadopoulos, G. Lombaert, and G. Degrande. The coupling loss of a building subject to railway induced vibrations: Numerical modelling and experimental measurements. *Journal of Sound and Vibration*, 442:459–481, 2019.

[36] L. G. Kurzweil. Ground-borne noise and vibration from underground rail systems. *Journal of Sound and Vibration*, 66(3):363–370, 1979.

[37] *Measurement and assessment of groundborne noise and vibration*, 2012. Association of Noise Consultants, 2nd ed.

[38] M. Villot, P. Jean, L. Grau, and S. Bailhache. Predicting railway-induced ground-borne noise from the vibration of radiating building elements using power-based building acoustics theory. *International Journal of Rail Transportation*, 6(1), 2018.

[39] R. A. Hood, R. J. Greer, M. Breslin, and P. R. Williams. The calculation and assessment of ground-borne noise and perceptible vibration from trains in tunnels. *Journal of Sound and Vibration*, 193(1):215–225, 1996.

[40] H. Kuppelwieser and A. Ziegler. A tool for predicting vibration and structure-borne noise immissions caused by railways. *Journal of Sound and Vibration*, 193(1):261–267, 1996.

[41] C. Madshus, B. Bessason, and L. Hårvik. Prediction model for low frequency vibration from high speed railways on soft ground. *Journal of Sound and Vibration*, 193(1):195–203, 1996.

[42] B. O. Hardin and V. P. Drnevich. Shear modulus and damping in soils: Measurement and parameter effects. *ASCE J Soil Mech Found Div*, 98(SM6), 1972.

[43] P. A. Costa, R. Calçada, A. Silva Cardoso, and A. Bodare. Influence of soil non-linearity on the dynamic response of high-speed railway tracks. *Soil Dynamics and Earthquake Engineering*, 30(4):221–235, 2010.

[44] J. W. S Rayleigh. On waves propagated along the plane surface of an elastic solid. *Proceedings of the London Mathematical Society*, 17:4–11, 1887.

[45] J. D. Achenbach. *Wave propagation in elastic solids*, volume 16 of North-Holland Series in Applied Mathematics and Mechanics. North-Holland, Amsterdam, The Netherlands, 1973.

[46] S. Nazarian and M. R. Desai. Automated surface wave method: field testing. *Journal of Geotechnical Engineering, Proceedings of the ASCE*, 119(7):1094–1111, 1993.

[47] N. Haskell. The dispersion of surface waves on multilayered media. *Bulletin of the Seismological Society of America*, 73:17–43, 1953.

[48] W. T. Thomson. Transmission of elastic waves through a stratifed soil medium. *Journal of Applied Physics*, 21:81–93, 1950.

[49] E. Kausel and J. M. Roësset. Stiffness matrices for layered soils. *Bulletin of the Seismological Society of America*, 35(6):1743–1761, 1981.

[50] X. Sheng, C. J. C. Jones, and D. J. Thompson. A theoretical model for ground vibration from trains generated by vertical track irregularities. *Journal of Sound and Vibration*, 272(3-5):937–965, 2004.

[51] E. Kausel. *Fundamental solutions in elastodynamics: a compendium*. Cambridge University Press, New York, 2006.

[52] M. Schevenels, S. Franois, and G. Degrande. EDT: An elastodynamics toolbox for matlab. *Computers and Geosciences*, 35(8):1752–1754, 2009.

[53] D. Kim and J. Lee. Propagation and attenuation characteristics of various ground vibrations. *Soil Dynamics and Earthquake Engineering*, 19(2):115–126, 2000.

[54] G. J. Rix, C. G. Lai, and A.W. Spang Jr. In situ measurement of damping ratio using surface waves. *Journal of Geotechnical and Geoenvironmental Engineering*, 126(5):472–480, 2000.

[55] C. G. Lai, G. J. Rix, S. Foti, and V. Roma. Simultaneous measurement and inversion of surface wave dispersion and attenuation curves. *Soil Dynamics*

and *Earthquake Engineering*, 22(9-12):923–930, 2002.

[56] M. Schevenels, G. Lombaert, G. Degrande, and S. Franois. A probabilistic assessment of resolution in the SASW test and its impact on the prediction of ground vibrations. *Geophysical Journal International*, 172(1):262–275, 2008.

[57] S. A. Badsar, M. Schevenels, W. Haegeman, and G. Degrande. Determination of the material damping ratio in the soil from sasw tests using the half-power bandwidth method. *Geophysical Journal International*, 182(3):1493–1508, 2010.

[58] N. Triepaischajonsak, D. J. Thompson, C. J. C. Jones, J. Ryue, and J. A. Priest. Ground vibration from trains: Experimental parameter characterization and validation of a numerical model. *Journal of Rail and Rapid Transit*, 225(2):140–153, 2011.

[59] V. P. Drnevich, B. O. Hardin, and D. J. Shippy. Modulus and damping of soils by the resonant-column method. *ASTM Special Technical Publication*, pages 91–125, 1978.

[60] T. Iwasaki, F. Tatsuoka, and Y. Takagi. Shear moduli of sands under cyclic torsional shear loading. *Soils and Foundations*, 18(1):39–56, 1978.

[61] X. Sheng, C. J. C. Jones, and M. Petyt. Ground vibration generated by a load moving along a railway track. *Journal of Sound and Vibration*, 228(1):129–156, 1999.

[62] A. Ditzel, G. C. Herman, and G. G. Drijkoningen. Seismograms of moving trains: Comparison of theory and measurements. *Journal of Sound and Vibration*, 248(4):635–652, 2001.

[63] V. V. Krylov. Generation of ground vibrations by superfast trains. *Applied Acoustics*, 44(2):149–164, 1995.

[64] H. A. Dieterman and A. Metrikine. Equivalent stiffness of a half-space interacting with a beam. critical velocities of a moving load along the beam. *European Journal of Mechanics, A/Solids*, 15(1):67–90, 1996.

[65] H. A. Dieterman and A. Metrikine. Critical velocities of a harmonic load moving uniformly along an elastic layer. *Journal of Applied Mechanics, Transactions ASME*, 64(3):596–600, 1997.

[66] P. A. Costa, A. Colaço, R. Calçada, and A. S. Cardoso. Critical speed of railway tracks. detailed and simplified approaches. *Transportation Geotechnics*, 2:30–46, 2015.

[67] C. Madshus and A. M. Kaynia. High-speed railway lines on soft ground: dynamic behaviour at critical train speed. *Journal of Sound and Vibration*, 231(3):689–701, 2000.

[68] H. Takemiya. Simulation of track-ground vibrations due to a high-speed train: The case of X-2000 at Ledsgard. *Journal of Sound and Vibration*, 261(3):503–526, 2003.

[69] X. Sheng, C. J. C. Jones, and D. J. Thompson. A theoretical study on the influence of the track on train-induced ground vibration. *Journal of Sound and Vibration*, 272(3-5):909–936, 2004.

[70] A. M. Kaynia, C. Madshus, and P. Zackrisson. Ground vibration from high-speed trains: prediction and countermeasure. *Journal of Geotechnical and Geoenvironmental Engineering*, 126(6):531–537, 2000.

[71] G. Degrande and G. Lombaert. An efficient formulation of krylov's prediction model for train induced vibrations based on the dynamic reciprocity theorem. *Journal of the Acoustical Society of America*, 110(3 I):1379–1390, 2001.

[72] L. Auersch. The excitation of ground vibration by rail traffic: Theory of vehicle-track-soil interaction and measurements on high-speed lines. *Journal of Sound and Vibration*, 284(1-2):103–132, 2005.

[73] L. Auersch. Ground vibration due to railway traffic-the calculation of the effects of moving static loads and their experimental verification. *Journal of Sound and Vibration*, 293(3-5):599–610, 2006.

[74] S. H. Ju, H. T. Lin, and J. Y. Huang. Dominant frequencies of train-induced vibrations. *Journal of Sound and Vibration*, 319:247–259, 2009.

[75] D.R.M. Milne, L.M. Le Pen, D.J. Thompson, and W. Powrie. Properties of train load frequencies and their applications. *Journal of Sound and Vibration*, 397:123–140, 2017.

[76] G. Lombaert, G. Degrande, S. François, and D. J. Thompson. Ground-borne vibration due to railway traffic. *Proceedings of the 11th International Workshop on Railway Noise*, Notes on Numerical Fluid Mechanics and multidisciplinary Design 126:253–287, 2013.

[77] M. Germonpré, J. C. O. Nielsen, G. Degrande, and G. Lombaert. Contributions of longitudinal track unevenness and track stiffness variation to railway induced vibration. *Journal of Sound and Vibration*, 437:292–307, 2018.

[78] G. Kouroussis, D. P. Connolly, and O. Verlinden. Railway induced ground vibrations — a review of vehicle effects. *International Journal of Rail Transportation*, 2(2):69–110, 2014.

[79] P. A. Costa, R. Calçada, and A. S. Cardoso. Influence of train dynamic modelling strategy on the prediction of track–ground vibrations induced by railway traffic. *Journal of Rail and Rapid Transit*, 226(4):434–450, 2012.

[80] G. Kouroussis, D. P. Connolly, G. Alexandrou, and K. Vogiatzis. Railway ground vibrations induced by wheel and rail singular defects. *Vehicle System Dynamics*, 53(10):1500–1519, 2015.

[81] S. L. Grassie. Rail irregularities, corrugation and acoustic roughness: Characteristics, significance and effects of reprofiling. *Proceedings of the Institution of Mechanical Engineers, Part F: Journal of Rail and Rapid Transit*, 226(5):542–557, 2012.

[82] E. Ntotsios, D. Thompson, and M. Hussein. The effect of track load correlation on ground-borne vibration from railways. *Journal of Sound and Vibration*, 402:142–163, 2017.

[83] C. J. C. Jones and J. R. Block. Prediction of ground vibration from freight trains. *Journal of Sound and Vibration*, 193(1):205–213, 1996.

[84] X. Sheng, C. J. C. Jones, and M. Petyt. Ground vibration generated by a harmonic load acting on a railway track. *Journal of Sound and Vibration*, 225(1):3–28, 1999.

[85] A. Karlström and A. Boström. An analytical model for train-induced ground vibrations from railways. *Journal of Sound and Vibration*, 292(1-2):221–241, 2006.

[86] J. A. Forrest and H. E. M. Hunt. A three-dimensional tunnel model for calculation of train-induced ground vibration. *Journal of Sound and Vibration*, 294(4):678–705, 2006.

[87] A. C. Eringen and S. S. Suhubi. *Elastodynamics*, volume 2. Academic Press, 1975.

[88] J. Domínguez and R. Abascal. On fundamental solutions for the boundary integral equations method in static and dynamic elasticity. *Engineering Analysis*, 1(3):128–134, 1984.

[89] J. A. Forrest and H. E. M. Hunt. Ground vibration generated by trains in underground tunnels. *Journal of Sound and Vibration*, 294(4):706–736, 2006.

[90] M. F. M. Hussein and H. E. M. Hunt. A numerical model for calculating vibration from a railway tunnel embedded in a full-space. *Journal of Sound and Vibration*, 305(3):401–431, 2007.

[91] M. F. M. Hussein and H. E. M. Hunt. A numerical model for calculating vibration due to a harmonic moving load on a floating-slab track with discontinuous slabs in an underground railway tunnel. *Journal of Sound and Vibration*, 321:361–371, 2009.

[92] K. A. Kuo, H. E. M. Hunt, and M. F. M. Hussein. The effect of a twin tunnel on the propagation of ground-borne vibration from an underground railway. *Journal of Sound and Vibration*, 330(25):6203–6222, 2011.

[93] A. Clot, R. Arcos, J. Romeu, and T. Pmies. Dynamic response of a double-deck circular tunnel embedded in a full-space. *Tunnelling and Underground Space Technology*, 59:146–156, 2016.

[94] M. F. M. Hussein, S. François, M. Schevenels, H. E. M. Hunt, J. P. Talbot, and G. Degrande. The fictitious force method for efficient calculation of vibration from a tunnel embedded in a multi-layered half-space. *Journal of Sound and Vibration*, 333(25):6996–7018, 2014.

[95] X. Sheng, C. J. C. Jones, and D. J. Thompson. Ground vibration generated by a harmonic load moving in a circular tunnel in a layered ground. *Journal of Low Frequency Noise Vibration and Active Control*, 22(2):83–96, 2003.

[96] Z. Yuan, A. Bostrm, and Y. Cai. Benchmark solution for vibrations from a moving point source in a tunnel embedded in a half-space. *Journal of Sound and Vibration*, 387:177–193, 2017.

[97] C. He, S. Zhou, H. Di, P. Guo, and J. Xiao. Analytical method for calculation of ground vibration from a tunnel embedded in a multi-layered half-space. *Computers and Geotechnics*, 99:149–164, 2018.

[98] F. C. P. de Barros and J. E. Luco. Response of a layered viscoelastic half-space to a moving point load. *Wave Motion*, 19(2):189–210, 1994.

[99] J. Domínguez. *Boundary Elements in Dynamics*. Computational Mechanics Publications and Elsevier Applied Science, 1993.

[100] Y. B. Yang, H. H. Hung, and D. W. Chang. Train-induced wave propagation in layered soils using finite/infinite element simulation. *Soil Dynamics and Earthquake Engineering*, 23(4):263–278, 2003.

[101] G. Kouroussis, O. Verlinden, and C. Conti. Ground propagation of vibrations from railway vehicles using a finite/infinite-element model of the soil. *Proceedings of the Institution of Mechanical Engineers, Part F: Journal of Rail and Rapid Transit*, 223(4):405–413, 2009.

[102] D. Connolly, A. Giannopoulos, and M. C. Forde. Numerical modelling of ground borne vibrations from high speed rail lines on embankments. *Soil Dynamics and Earthquake Engineering*, 46:13–19, 2013.

[103] P. Lopes, P. A. Costa, M. Ferraz, R. Calçada, and A. S. Cardoso. Numerical modeling of vibrations induced by railway traffic in tunnels: From the source to the nearby buildings. *Soil Dynamics and Earthquake Engineering*, 61-62:269–285, 2014.

[104] C. J. C. Jones, D. J. Thompson, and M. Petyt. A model for ground vibration from railway tunnels. *Proceedings of the Institution of Civil Engineers: Transport*, 153(2):121–129, 2002.

[105] A. Garcia-Bennett, C. J. C. Jones, and D. J. Thompson. A numerical investigation of railway ground vibration mitigation using a trench in a layered soil. *Notes on Numerical Fluid Mechanics and Multidisciplinary Design*, 118:315–322, 2012.

[106] L. Andersen and C. J. C. Jones. Coupled boundary and finite element analysis of vibration from railway tunnels-a comparison of two- and three-dimensional models. *Journal of Sound and Vibration*, 293(3-5):611–625, 2006.

[107] Y. B. Yang and H. H. Hung. A 2.5D finite/infinite element approach for mod-

elling visco-elastic bodies subjected to moving loads. *International Journal for Numerical Methods in Engineering*, 51(11):1317–1336, 2001.

[108] Y. B. Yang and H. H. Hung. Soil vibrations caused by underground moving trains. *Journal of Geotechnical and Geoenvironmental Engineering*, 134(11):1633–1644, 2008.

[109] Y. B. Yang, X. Liang, H. H. Hung, and Y. Wu. Comparative study of 2D and 2.5D responses of long underground tunnels to moving train loads. *Soil Dynamics and Earthquake Engineering*, 97:86–100, 2017.

[110] P. Jean, C. Guigou, and M. Villot. A 2.5D BEM model for ground-structure interaction. *Building Acoustics*, 11(3):157–173, 2004.

[111] M. Villot, P. Ropars, P. Jean, E. Bongini, and F. Poisson. Modeling the influence of structural modifications on the response of a building to railway vibration. *Noise Control Engineering Journal*, 59(6):641–651, 2011.

[112] X. Sheng, C. J. C. Jones, and D. J. Thompson. Modelling ground vibration from railways using wavenumber finite- and boundary-element methods. *Proceedings of the Royal Society A: Mathematical, Physical and Engineering Sciences*, 461(2059):2043–2070, 2005.

[113] X. Sheng, C. J. C. Jones, and D. J. Thompson. Prediction of ground vibration from trains using the wavenumber finite and boundary element methods. *Journal of Sound and Vibration*, 293(3-5):575–586, 2006.

[114] Q. Jin, D. J. Thompson, D. E. J. Lurcock, M. G. R. Toward, and E. Ntotsios. A 2.5D finite element and boundary element model for the ground vibration from trains in tunnels and validation using measurement data. *Journal of Sound and Vibration*, 422:373–389, 2018.

[115] G. Lombaert and G. Degrande. Ground-borne vibration due to static and dynamic axle loads of intercity and high-speed trains. *Journal of Sound and Vibration*, 319:1036–1066, 2009.

[116] P. Galvín, S. François, M. Schevenels, E. Bongini, G. Degrande, and G. Lombaert. A 2.5D coupled FE-BE model for the prediction of railway induced vibrations. *Soil Dynamics and Earthquake Engineering*, 30(12):1500–1512, 2010.

[117] P. Galvín, A. Romero, and J. Domínguez. Vibrations induced by HST passage on ballast and non-ballast tracks. *Soil Dynamics and Earthquake Engineering*, 30(9):862–873, 2010.

[118] P. Alves Costa, R. Calçada, and A. Silva Cardoso. Track-ground vibrations induced by railway traffic: In-situ measurements and validation of a 2.5D FEM-BEM model. *Soil Dynamics and Earthquake Engineering*, 32(1):111–128, 2012.

[119] A. Dijckmans, P. Coulier, J. Jiang, M. G. R. Toward, D. J. Thompson, G. Degrande, and G. Lombaert. Mitigation of railway induced ground vibration by heavy masses next to the track. *Soil Dynamics and Earthquake Engineering*, 75:158–170, 2015.

[120] D. J. Thompson, J. Jiang, M. G. R. Toward, M. F. M. Hussein, E. Ntotsios, A. Dijckmans, P. Coulier, G. Lombaert, and G. Degrande. Reducing railway-induced ground-borne vibration by using open trenches and soft-filled barriers. *Soil Dynamics and Earthquake Engineering*, 88:45–59, 2016.

[121] P. Amado-Mendes, P. Alves Costa, L. M. C. Godinho, and P. Lopes. 2.5D MFS-FEM model for the prediction of vibrations due to underground railway traffic. *Engineering Structures*, 104:141–154, 2015.

[122] A. Yaseri, M. H. Bazyar, and S. Javady. 2.5D coupled FEM-SBFEM analysis of ground vibrations induced by train movement. *Soil Dynamics and Earthquake Engineering*, 104:307–318, 2018.

[123] L. Auersch. Dynamics of the railway track and the underlying soil: the boundary-element solution, theoretical results and their experimental verification. *Vehicle System Dynamics*, 43(9):671–695, 2005.

[124] L. Auersch. Vehicle-track-interaction and soil dynamics. *Vehicle System Dynamics*, 29(SUPPL.):553–558, 1998.

[125] G. Degrande, D. Clouteau, R. Othman, M. Arnst, H. Chebli, R. Klein, P. Chatterjee, and B. Janssens. A numerical model for ground-borne vibrations from underground railway traffic based on a periodic finite element-boundary element formulation. *Journal of Sound and Vibration*, 293(3-5):645–666, 2006.

[126] P. Ropars, X. Vuylsteke, and E. Augis. Vibrations induced by metro in sensitive buildings; experimental and numerical comparisons. In M. Taroudakis, editor, *EURONOISE 2018 Conference*, pages 1381–1386, Heraklion, Greece, 2018.

[127] P. Jean. A 2.75D model for the prediction of noise inside buildings due to train traffic. *Acta Acustica united with Acustica*, 104(6):1009–1018, 2018.

[128] P. Fiala, G. Degrande, and F. Augusztinovicz. Numerical modelling of ground-borne noise and vibration in buildings due to surface rail traffic. *Journal of Sound and Vibration*, 301(3-5):718–738, 2007.

[129] M. Hussein, H. Hunt, K. Kuo, P. A. Costa, and J. Barbosa. The use of sub-modelling technique to calculate vibration in buildings from underground railways. *Proceedings of the Institution of Mechanical Engineers, Part F: Journal of Rail and Rapid Transit*, 229(3):303–314, 2015.

[130] P. Galvín, A. Romero, and J. Domínguez. Fully three-dimensional analysis of high-speed train-track-soil-structure dynamic interaction. *Journal of Sound and Vibration*, 329(24):5147–5163, 2010.

[131] H. Xia, Y. M. Cao, and G. De Roeck. Theoretical modeling and characteristic analysis of moving-train induced ground vibrations. *Journal of Sound and Vibration*, 329(7):819–832, 2010.

[132] J. Y. Shih, D. J. Thompson, and A. Zervos. The influence of soil nonlinear properties on the track/ground vibration induced by trains running on soft ground. *Transportation Geotechnics*, 11:1–16, 2017.

[133] J. Y. Shih, D. J. Thompson, and A. Zervos. The effect of boundary conditions, model size and damping models in the finite element modelling of a moving load on a track/ground system. *Soil Dynamics and Earthquake Engineering*, 89:12–27, 2016.

[134] L. Hall. Simulations and analyses of train-induced ground vibrations in finite element models. *Soil Dynamics and Earthquake Engineering*, 23:403–413, 2003.

[135] H. Lane, T. Ekevid, P. Kettil, C. Y. Ching, and N. E. Wiberg. Vehicle-track-underground modeling of rail induced wave propagation. *Computers and Structures*, 85(15-16):1215–1229, 2007.

[136] A. El Kacimi, P. K. Woodward, O. Laghrouche, and G. Medero. Time domain 3D finite element modelling of train-induced vibration at high speed. *Computers and Structures*, 118:66–73, 2013.

[137] Q. Fu and C. Zheng. Three-dimensional dynamic analyses of track-embankment-ground system subjected to high speed train loads. *The Scientific World Journal*, 2014, 2014.

[138] H. Lane, P. Kettil, and N. E. Wiberg. Moving finite elements and dynamic vehicle interaction. *European Journal of Mechanics, A/Solids*, 27(4):515–531, 2008.

[139] N. Triepaischajonsak and D. J. Thompson. A hybrid modelling approach for

predicting ground vibration from trains. *Journal of Sound and Vibration*, 335:147–173, 2015.

[140] S. G. Koroma, D. J. Thompson, M. F. M. Hussein, and E. Ntotsios. A mixed space-time and wavenumber-frequency domain procedure for modelling ground vibration from surface railway tracks. *Journal of Sound and Vibration*, 400:508–532, 2017.

[141] J. C.O. Nielsen, G. Lombaert, and S. François. A hybrid model for prediction of ground-borne vibration due to discrete wheel/rail irregularities. *Journal of Sound and Vibration*, 345:103–120, 2015.

[142] K. A. Kuo, H. Verbraken, G. Degrande, and G. Lombaert. Hybrid predictions of railway induced ground vibration using a combination of experimental measurements and numerical modelling. *Journal of Sound and Vibration*, 373:263–284, 2016.

[143] G. Kouroussis, K.E. Vogiatzis, and D. P. Connolly. Assessment of railway ground vibration in urban area using in-situ transfer mobilities and simulated vehicle-track interaction. *International Journal of Rail Transportation*, 6(2):113–130, 2018.

[144] G. Kouroussis, D. P. Connolly, M. C. Forde, and O. Verlinden. Train speed calculation using ground vibrations. *Journal of Rail and Rapid Transit*, 229(5):466–483, 2015.

[145] D. J. Thompson. *Railway Noise and Vibration: Mechanisms, Modelling and Means of Control.* Elsevier, Oxford, U.K., 1st edition, 2008.

[146] G. Kouroussis, O. Verlinden, and C. Conti. On the interest of integrating vehicle dynamics for the ground propagation of vibrations: the case of urban railway traffic. *Vehicle System Dynamics*, 48(12):1553–1571, 2010.

[147] J. C. O. Nielsen, A. Mirza, S. Cervello, P. Huber, R. Müller, B. Nelain, and P. Ruest. Reducing train-induced ground-borne vibration by vehicle design and maintenance. *International Journal of Rail Transportation*, 3(1):17–39, 2015.

[148] A. A. Mirza, A. Frid, J. C. O. Nielsen, and C. J. C. Jones. *Ground vibration induced by railway traffic - The influence of vehicle parameters*, volume 118 of *Notes on Numerical Fluid Mechanics and Multidisciplinary Design.* Nagahama, Japan, 2012.

[149] G. Kouroussis, O. Verlinden, and C. Conti. Efficiency of resilient wheels on the alleviation of railway ground vibrations. *Journal of Rail and Rapid Transit*, 226(4):381–396, 2012.

[150] G. Alexandrou, G. Kouroussis, and O. Verlinden. A comprehensive prediction model for vehicle/track/soil dynamic response due to wheel flats. *Journal of Rail and Rapid Transit*, 230(4):1088–1104, 2016.

[151] G. Kouroussis, D. P. Connolly, G. Alexandrou, and K. Vogiatzis. The effect of railway local irregularities on ground vibration. *Transportation Research — Part D: Transport and Environment*, 39:17–30, 2015.

[152] G. Kouroussis, O. Verlinden, and C. Conti. Influence of some vehicle and track parameters on the environmental vibrations induced by railway traffic. *Vehicle System Dynamics*, 50(4):619–639, 2012.

[153] A. V. Metrikine, A. V. Vostrukhov, and A. C. W. M. Vrouwenvelder. Drag experienced by a high-speed train due to excitation of ground vibrations. *International Journal of Solid and Structure*, 38:8851–8868, 2001.

[154] A. V. Vostroukhov and A. V. Metrikine. Periodically supported beam on a visco-elastic layer as a model for dynamic analysis of a high-speed railway track. *International Journal of Solids and Structures*, 40(21):5723–5752, 2003.

[155] D. Thompson, X. Zhang, E. Ntotsios, and G. Squicciarini. A comparison of the noise and vibration performance of slab and ballasted track designs. In *Railways 2018, The Fourth International Conference on Railway Technology*, Sitges, Barcelona, Spain, 3-7 September 2018.

[156] D. P. Connolly, G. Kouroussis, O. Laghrouche, C. Ho, and M. C. Forde. Benchmarking railway vibrations — track, vehicle, ground and building effects. *Construction and Building Materials*, 92:64–81, 2015.

[157] D. Connolly, A. Giannopoulos, and M. C. Forde. Numerical modelling of ground borne vibrations from high speed rail lines on embankments. *Soil Dynamics and Earthquake Engineering*, 46:13–19, 2013.

[158] B. Olivier, D. P. Connolly, P. Alves Costa, and G. Kouroussis. The effect of embankment on high speed rail ground vibrations. *International Journal of Rail Transportation*, 4(4):229–246, 2016.

[159] G. A. Athanasopoulos, P. C. Pelekis, and G. A. Anagnostopoulos. Effect of soil stiffness in the attenuation of Rayleigh-wave motions from field measurements. *Soil Dynamics and Earthquake Engineering*, 19(3):277–288, 2000.

[160] G. Kouroussis, C. Conti, and O. Verlinden. Investigating the influence of soil properties on railway traffic vibration using a numerical model. *Vehicle System Dynamics*, 51(3):421–442, 2013.

[161] L. Auersch and S. Said. Attenuation of ground vibrations due to different technical sources. *Earthquake Engineering and Engineering Vibration*, 9:337–344, 2010.

[162] J. Y. Shih, D. J. Thompson, and E. Ntotsios. Analysis of resonance effect for a railway track on a layered ground. *Transportation Geotechnics*, 16:51–62, 2018.

[163] G. Degrande, G. De Roeck, W. Dewulf, P. Van den Broeck, and M. Verlinden. Design of a vibration isolating screen. In P. Sas, editor, *Proceedings ISMA 21, Noise and Vibration Engineering, Vol. II*, pages 823–834, Leuven (Belgium), 1996.

[164] D. Connolly, A. Giannopoulos, W. Fan, P.K. Woodward, and M.C. Forde. Optimising low acoustic impedance back-fill material wave barrier dimensions to shield structures from ground borne high speed rail vibrations. *Construction and Building Materials*, 44:557–564, 2013.

[165] A. Garinei, G. Risitano, and L. Scappaticci. Experimental evaluation of the efficiency of trenches for the mitigation of train-induced vibrations. *Transportation Research Part D: Transport and Environment*, 32(0):303–315, 2014.

[166] P. Coulier, S. François, G. Degrande, and G. Lombaert. Subgrade stiffening next to the track as a wave impeding barrier for railway induced vibrations. *Soil Dynamics and Earthquake Engineering*, 48:119–131, 2013.

[167] D. J. Thompson, J. Jiang, M. G. R. Toward, M. F. M. Hussein, A. Dijckmans, P. Coulier, G. Degrande, and G. Lombaert. Mitigation of railway-induced vibration by using subgrade stiffening. *Soil Dynamics and Earthquake Engineering*, 79:89–103, 2015.

[168] P. Coulier, G. Degrande, A. Dijckmans, J. Houbrechts, G. Lombaert, W. Rücker, L. Auersch, M. R. Plaza, V. Cuellar, D. Thompson, A. Ekblad, and A. Smekal. Scope of the parametric study on mitigation measures on the transmission path. Technical report, RIVAS project SCP0-GA-2010-265754, Deliverable D4.1, Report to the EC, October 2011.

[169] M. Sanayei, P. Maurya, and J. A. Moore. Measurement of building foundation and ground-borne vibrations due to surface trains and subways. *Engineering Structures*, 53:102–111, 2013.

[170] H. Mouzakis and K. Vogiatzis. Ground-borne noise and vibration trans-

mitted from subway networks to multi-storey reinforced concrete buildings. *Transport*, 33(2)):446–453, 2018.

[171] D. Ulgen, O. L. Ertugrul, and M. Y. Ozkan. Measurement of ground borne vibrations for foundation design and vibration isolation of a high-precision instrument. *Measurement*, 93:385–396, 2016.

[172] J. P. Talbot. Base-isolated buildings: towards performance-based design. *Proceedings of the Institution of Civil Engineers — Structures and Buildings*, 169(8):574–582, 2016.

[173] S. Kaewunruen and V. Martin. Life cycle assessment of railway ground-borne noise and vibration mitigation methods using geosynthetics, metamaterials and ground improvement. *Sustainability*, 10(10):3753, 2018.

[174] A. Paixão, E. Fortunato, and R. Calçada. Design and construction of backfills for railway track transition zones. *Journal of Rail and Rapid Transit*, 229(1):58–70, 2015.

[175] M. Germonpré, G. Degrande, and G. Lombaert. Periodic track model for the prediction of railway induced vibration due to parametric excitation. *Transportation Geotechnics*, 17:98–108, 2018.

[176] P. Wang, K. Wei, Y. Liang, and F. Wang. Experimental investigation of the vibration-attenuating effect of rail suspension fasteners on environment vibration induced by subway. *Journal of Vibroengineering*, 18(6):3956–3969, 2016.

[177] K. Vogiatzis. Protection of the cultural heritage from underground metro vibration and ground-borne noise in Athens centre: The case of the Kerameikos archaeological museum and Gazi cultural centre. *International Journal of Acoustics and Vibration*, 17:59–72, 2012.

[178] K. Vogiatzis, V. Zafiropoulou, and H. Mouzakis. Monitoring and assessing the effects from metro networks construction on the urban acoustic environment: The Athens Metro line 3 extension. *Science of The Total Environment*, 639:1360–1380, 2018.

[179] S. Zhu, J. Yang, C. Cai, Z. Pan, and W. Zhai. Application of dynamic vibration absorbers in designing a vibration isolation track at low-frequency domain. *Journal of Rail and Rapid Transit*, 231(5):546–557, 2017.

[180] S. Zhu, J. Wang, C. Cai, K. Wang, W. Zhai, J. Yang, and H. Yan. Development of a vibration attenuation track at low frequencies for urban rail transit. *Computer-Aided Civil and Infrastructure Engineering*, 32(9):713–726, 2017.

[181] Z. Chen, H. Fang, Z. Han, and S. Sun. Influence of bridge-based designed TMD on running trains. *Journal of Vibration and Control*, in press (doi: 10.1177/1077546318773022):1–12, 2018.

[182] J. Xu, P. Wang, X. Ma, Y. Gao, and R. Chen. Stiffness characteristics of high-speed railway turnout and the effect on the dynamic train-turnout interaction. *Shock and Vibration*, article ID 1258681:14 pages, 2016.

[183] S. Bruni, I. Anastasopoulos, S. Alfi, A. Van Leuven, M. Apostolou, and G. Gazetas. Train–induced vibrations on urban metro and tram turnouts. *Journal of Transportation Engineering*, 135(7):397–405, 2009.

[184] N. K. Mandal, M. Dhanasekar, and Y. Q. Sun. Impact forces at dipped rail joints. *Journal of Rail and Rapid Transit*, 230(1):271–282, 2016.

[185] R. U. A. Uzzal, W. Ahmed, and R. B. Bhat. A three-dimensional modeling study of wheel/rail impacts created by multiple wheel flats, and the development of a smart wheelset. *Journal of Rail and Rapid Transit*, 230(2):450–471, 2016.

[186] I. Grossoni, S. Iwnicki, Y. Bezin, and C. Gong. Dynamics of a vehicle–track coupling system at a rail joint. *Journal of Rail and Rapid Transit*,

229(4):364–374, 2015.

[187] J. P. Talbot. Lift-over crossings as a solution to tram-generated ground-borne vibration and re-radiated noise. *Journal of Rail and Rapid Transit*, 228(8):878–886, 2014.

[188] J. Nielsen, A. Mirza, S. Cervello, P. Huber, R. Müller, B. Nelain, and P. Ruest. Reducing train-induced ground-borne vibration by vehicle design and maintenance. *International Journal of Rail Transportation*, 3(1):17–39, 2015.

[189] G. Kouroussis, S. Zhu, B. Olivier, D. Ainalis, and W. Zhai. Urban railway ground vibrations induced by localized defects: using dynamic vibration absorbers as a mitigation solution. *Journal of Zhejiang University — Science A*, 20(2):83–97, 2019.

[190] Hans-Joerg Terno. State of the art review of mitigation measures on track. *RIVAS project, SCP0-GA-2010-265754*, Report to the EC (Deliverable D3.1), 2012.

[191] A. Johansson, J. C. O. Nielsen, R. Bolmsvik, A. Karlström, and R. Lundén. Under sleeper pads — influence on dynamic train–track interaction. *Wear*, 265(9-10):1479–1487, 2008.

[192] R. Verachtert, H. E. M. Hunt, M. F. M. Hussein, and G. Degrande. Changes of perceived unevenness caused by in-track vibration countermeasures in slab track. *European Journal of Mechanics, A/Solids*, 65, 2017.

[193] L. Auersch. Dynamic axle loads on tracks with and without ballast mats: numerical results of three-dimensional vehicle-track-soil models. *Journal of Rail and Rapid Transit*, 220(2):169–183, 2006.

[194] P. Alves Costa, R. Calada, and A. Silva Cardoso. Ballast mats for the reduction of railway traffic vibrations. numerical study. *Soil Dynamics and Earthquake Engineering*, 42:137–150, 2012.

[195] M. Sol-Sánchez, F. Moreno-Navarro, and M. C. Rubio-Gámez. The use of elastic elements in railway tracks: A state of the art review. *Construction and Building Materials*, 75:293–305, 2015.

[196] P. M. Fernãndez, I. V. Sanchãs, F. B. Rojas, and R. I. Franco. Monitoring and analysis of vibration transmission for various track typologies. a case study. *Transportation Research Part D: Transport and Environment*, 24:98–109, 2013.

[197] E. Bongini, R. Müller, R. Garburg, and A. Pieringer. Design guide and technology assessment of the track mitigation measures. *RIVAS project, SCP0-GA-2010-265754*, Report to the EC(Deliverable D3.13), 2012.

[198] P. Grootenhuis. Floating track slab isolation for railways. *Journal of Sound and Vibration*, 51(3):443–448, 1977.

[199] H. Hunt and M. Hussein. Vibration from railways: can we achieve better than ±10 dB accuracy? In *14th International Congress on Sound and Vibration*, Cairns, Australia, July 2007.

[200] D. P. Connolly, G. Kouroussis, A. Giannopoulos, O. Verlinden, P. K. Woodward, and M. C. Forde. Assessment of railway vibrations using an efficient scoping model. *Soil Dynamics and Earthquake Engineering*, 58:37–47, 2014.

[201] D. P. Connolly, G. Kouroussis, P. K. Woodward, O. Verlinden, A. Giannopoulos, and M. C. Forde. Scoping prediction of re-radiated ground-borne noise and vibration near high speed rail lines with variable soils. *Soil Dynamics and Earthquake Engineering*, 66:78–88, 2014.

[202] A. Castanheira-Pinto, P. Alves-Costa, L. Godinho, and P. Amado-Mendes. On the application of continuous buried periodic inclusions on the filtering of traffic vibrations: A numerical study. *Soil Dynamics and Earthquake Engineering*, 113:391–405, 2018.

[203] M. Villot, S. Bailhache, C. Guigou, and P. Jean. Prediction of railway in-
duced vibration and ground borne noise exposure in buildings and associated
annoyance. In *Proceedings of the the 11th International Workshop on Rail-
way Noise (IWRN11)*, volume 126 of *Notes on Numerical Fluid Mechanics
and Multidisciplinary Design*, pages 289–296, Uddevalla, Sweden, 2015.